Earth Syst. Sci. Data, 18, 1833–1854, 2026
https://doi.org/10.5194/essd-18-1833-2026

Open Access Earth System Science Data

RAPSODI: radiosonde atmospheric profiles from ship and island platforms during ORCESTRA, collected to Decipher the ITCZ

Marius Winkler[1], Marius Rixen[1], Florent Beucher[2], Fleur Couvreux[2], Chaehyeon C. Nam[3], Philippe Peyrillé[2], Hauke Schmidt[1], Hans Segura[1], Karl-Hermann Wieners[1], Ezri Alkilani-Brown[4,★], Abdou Aziz Coly[5,★], Giovanni Biagioli[6,★], Michael M. Bell[7,★], Ester Brito[8,★], Emma Chauvin[2,★], Julie Capo[2,★], Delián Colón-Burgos[7,★], Akeem Dawes[9,★], Jose Carlos da Luz[8,★], Zekican Demiralay[16,★], Vincent Douet[10,★], Vincent Ducastin[2,★], Clarisse Dufaux[6,★], Jean-Louis Dufresne[6,★], Florence Favot[2,★], Thomas Fiolleau[11,★], Emilie Fons[6,★], Geet George[12,★], Helene M. Gloeckner[1,★], Suelly Gonçalves[12,★], Laurent Gouttesoulard[11,★], Lennéa Hayo[1,★], Wei-Ting Hsiao[3,★], Sarah Kennison[3,★], Michael Kopelman[3,★], Tsung-Yung Lee[3,★], Enora Le Gall[6,★], Mateo Lovato[13,★], Emily Luschen[14,★], Nicolas Maury[6,★], Brett McKim[6,★], Louis Netz[11,★], Diouf Ousseynou[5,★], Karsten Peters-von Gehlen[18,★], Chavez Pope[9,★], Basile Poujol[6,★], Niwde Rivera Maldonado[15,★], Nina Robbins-Blanch[19,★], Nicolas Rochetin[6,★], Daniel Rowe[9,★], Paula Romero Jure[4,★], James H. Ruppert Jr.[14,★], Jairo Segura Bermudez[1,★], Jarrett C. Starr[3,★], Martin Stelzner[17,★], Connor Stoll[3,★], Macintyre Syrett[14,★], Abraham Tekoe[3,★], Jeremie Trules[10,★], Colin Welty[14,★], Daniel Klocke[1], Raphaela Vogel[19], Sandrine Bony[6], Allison A. Wing[3], and Bjorn Stevens[1]

[1]Max-Planck-Institut für Meteorologie, Hamburg, Germany
[2]Centre National de Recherches Météorologiques, University of Toulouse, Météo-France, CNRS, Toulouse, France
[3]Department of Earth, Ocean and Atmospheric Science, Florida State University, Tallahassee, FL, USA
[4]School of Earth and Environment, University of Leeds, Leeds, United Kingdom
[5]Agence Nationale de l'Aviation Civile et de la Météorologie, Dakar, Sénégal
[6]Laboratoire de Météorologie Dynamique/IPSL, Sorbonne Université, École Normale Supérieure, École Polytechnique, CNRS, Paris, France
[7]Department of Atmospheric Science, Colorado State University, Fort Collins, CO, USA
[8]Instituto Nacional de Meteorologia e Geofísica, Sal, Cape Verde
[9]Caribbean Institute for Meteorology and Hydrology, Bridgetown, Barbados
[10]Institute Pierre-Simon Laplace, CNRS, Paris, France
[11]Laboratoire d'Etudes en Geophysique et Océanographie Spatiale, University of Toulouse, IRD, CNRS, CNES, UPS, Toulouse, France
[12]Department of Geoscience and Remote Sensing, Delft University of Technology, Delft, the Netherlands
[13]Department of Electrical and Computer Engineering, Colorado State University, Fort Collins, CO, USA
[14]School of Meteorology, University of Oklahoma, Norman, OK, USA
[15]University of Puerto Rico, Mayagüez, Puerto Rico
[16]Meteorological Institute, Ludwig Maximilian University, Munich, Germany
[17]Deutscher Wetterdienst, Offenbach, Germany
[18]Deutsches Klimarechenzentrum GmbH, Hamburg, Germany
[19]Universität Hamburg, Hamburg, Germany
★These authors contributed equally to this work.

Correspondence: Marius Winkler (marius.winkler@mpimet.mpg.de)

Published by Copernicus Publications.

Received: 29 October 2025 – Discussion started: 20 November 2025
Revised: 26 February 2026 – Accepted: 26 February 2026 – Published: 11 March 2026

Abstract. The RAPSODI (Radiosonde Atmospheric Profiles from Ship and island platforms during ORCESTRA, collected to Decipher the ITCZ) radiosonde dataset was collected during the ORCESTRA field campaign in August and September 2024. It is designed to investigate the mechanisms linking mesoscale tropical convection to tropical waves and to air-sea heat and moisture exchanges that regulate convection and tropical cyclone formation. The campaign began at the Instituto Nacional de Meteorologia e Geofísica (INMG) on Sal in the Cape Verde Islands, continued with ship-based observations aboard the German research vessel R/V *Meteor* during an Atlantic transect, and concluded at the Barbados Cloud Observatory (BCO) in the eastern Caribbean. Over the 52 d campaign, a total of 624 radiosondes were launched at high temporal frequency (typically every three hours), capturing high-resolution vertical profiles of temperature, humidity, pressure, and winds from three complementary platforms. The dataset encompasses raw, quality-controlled, and vertically gridded data, is detailed in this paper and offers a valuable resource for investigating the atmospheric structure and processes shaping tropical convection and the intertropical convergence zone (ITCZ). The datasets generated in this study include raw radiosonde measurements (Level 0), oscillating and merged radiosonde profiles (Level 1), and vertically gridded profiles (Level 2), which are publicly available via the ORCESTRA data portal and DOI-referenced archives (Winkler et al., 2025a; https://ipfs.io/ipns/latest.orcestra-campaign.org/raw/BCO/radiosondes/, Winkler et al., 2025b; https://ipfs.io/ipns/latest.orcestra-campaign.org/raw/INMG/radiosondes/, Winkler et al., 2025c; https://ipfs.io/ipns/latest.orcestra-campaign.org/raw/METEOR/radiosondes/, Winkler et al., 2025d; https://doi.org/10.82246/BAFYBEIHXRAJOJUQZYX65QSO7AMA6NGVREETKDW3HQZX3SDZFB7LCMG6VAQ, Winkler et al., 2026; https://doi.org/10.82246/BAFYBEIA34AUWYVBH2RQ7CN7AGUZZ7PULQ2KRDDDIEESM6KPYSI, Winkler and Rixen, 2026a; https://doi.org/10.82246/BAFYBEID7CNW62ZMZFGXCVC6Q6FA267A7IVK2W, Winkler and Rixen, 2026b).

1 Introduction

The ORganized Convection and EarthCare Studies over the TRopical Atlantic (ORCESTRA) campaign is an international field study aimed at advancing the understanding of tropical meteorology and atmospheric processes (Stevens et al., 2026). The overall objectives of ORCESTRA are (i) to determine the drivers of mesoscale organisation in the tropics and their impact on small-scale weather systems and the large-scale circulation, with a particular focus on the structure and variability of the Atlantic ITCZ, and (ii) to serve as a benchmark for satellite remote sensing and a new generation of high-resolution storm-resolving models. The campaign brought together several coordinated subcampaigns targeting complementary aspects of tropical convection and air–sea interaction, including those contributing to the radiosonde observations (Table 1). Aircraft-based activities focused on convective organization, while ship-based experiments aboard the German research vessel R/V *Meteor* investigated ocean–atmosphere coupling and mesoscale convection. Additional observations at the Barbados Cloud Observatory targeted sub-cloud processes. Through this coordinated, multi-platform effort, radiosondes were launched across the tropical Atlantic from Sal in the east to Barbados in the west, complemented by ship-borne measurements aboard the R/V *Meteor*. A comprehensive overview paper of the ORCESTRA campaign is currently in preparation and will place ORCESTRA in the broader historical context of Atlantic radiosonde observations, including previous ship-based efforts.

Radiosondes, which are a central tool for observing the vertical structure of the tropical atmosphere, were included in each of the subcampaigns mentioned above, as all contributed to their funding. They had long been an essential tool for profiling the atmosphere (Lettau, 1950), but the first large-scale coordinated use in an international campaign came with the GARP Atlantic Tropical Experiment (GATE) in 1974 (Mason, 1975), after which they became indispensable for characterizing atmospheric profiles in field studies. When launched frequently across multiple platforms, radiosondes enable analyses of thermodynamic profiles, wind patterns, and moisture convergence on meso- and synoptic scales. Such networks have supported progress in understanding cloud–circulation coupling, as demonstrated by EUREC^{4}A (Stephan et al., 2021), where coordinated radiosonde launches captured the rapid deepening and moistening of the boundary layer during the passage of a characteristic "fish" cloud pattern (their Fig. 10). This episode marked a transition from shallow to deeper convection, accompanied by a pronounced reorganization of humidity and pressure structures which is an example of how sustained radiosonde observations can reveal the evolving coupling

Table 1. ORCESTRA subcampaigns contributing to the radiosonde observations and their scientific focus. Other ORCESTRA subcampaigns did not participate in the radiosonde mission and are therefore not listed.

Acronym	Full name and primary focus
PERCUSION	Persistent EarthCare Underflight Studies of the ITCZ and Organized Convection
MAESTRO	Mesoscale organisation of tropical convection
BOWTIE	Beobachtung von Ozean und Wolken – das Trans ITCZ Experiment
PICCOLO	Process Investigation of Clouds and Convective Organization over the AtLantic Ocean
SCORE	Sub-Cloud Observations of Rain Evaporation

between mesoscale convection and the large-scale environment. The ORCESTRA campaign builds on this approach, extending sounding observations across the tropical Atlantic, including both within and at the edge of the ITCZ, and providing continuous time–height measurements during day and night.

Over the 52 d campaign, radiosondes were launched at high temporal frequency from three platforms: the Instituto Nacional de Meteorologia e Geofísica (INMG) on Sal Island, Cape Verde, the R/V *Meteor* during its Atlantic transect, and the Barbados Cloud Observatory (BCO) in the western Atlantic. These profiles complement measurements from other platforms, including cloud observations from remote sensing instruments on the R/V *Meteor* and dropsondes released from the HALO aircraft (Gloeckner et al., 2026) by offering higher maximum height, the possibility of obtaining both ascent and descent profiles from a single launch, and continuous 3-hourly coverage including at night. In the central Atlantic, where dropsonde coverage is absent, the many R/V *Meteor* profiles provide unique sampling. Together, these complementary datasets enable multi-scale studies of convection, tropical wave activity, and air–sea interaction.

The radiosondes from the three platforms (BCO, INMG and R/V *Meteor*) are aggregated into a unified dataset called RAPSODI. The different platforms are described in Sect. 2. Section 3 outlines the data acquisition and the data processing methods, while Sect. 4 discusses the observed atmospheric conditions. Finally, the paper presents the code and data availability before concluding with a summary.

2 The ORCESTRA sounding network

This section describes the ORCESTRA radiosonde network, its sampling strategy, and its measurement setups. Over the course of the campaign (Stevens et al., 2026), a total of 624 radiosondes were launched from three platforms spanning the tropical Atlantic. Here, we use ascent and descent to denote the two branches of a single balloon-launched radiosonde flight; the descent branch is recorded after balloon burst (parachute-assisted where applicable) and should not be confused with aircraft-deployed dropsondes. The stationary sites at INMG and BCO provided repeated profiles at fixed locations, while the R/V *Meteor* contributed time-dependent profiles along its transect from the eastern to the western Atlantic.

In the following, the three launch platforms and their respective measurement setups are described in more detail. To illustrate the diversity of observing strategies within ORCESTRA, the radiosonde launches are grouped by their platform and associated subcampaigns:

1. as part of MAESTRO from the INMG at Aeroporto Amílcar Cabral, Sal Island, Republic of Cabo Verde,
2. as part of BOWTIE and PICCOLO from the Research Vessel Meteor (Klocke et al., 2026) which crossed the Atlantic from east to west, and
3. in coordination with PERCUSION, SCORE and PICCOLO from the Barbados Cloud Observatory at Deebles Point, St. Philip, Barbados (Stevens et al., 2016).

Figure 1 illustrates the radiosonde launch platforms and trajectories. The ship campaign began in the eastern Atlantic at the port of Mindelo on São Vicente Island, Cape Verde, and concluded in the western Atlantic at the port of Bridgetown, Barbados.

Radiosondes were launched between 9 August and 29 September from the three different platforms as illustrated in Fig. 2. Of the ascending profiles, 91 % were successfully tracked during descent, and 48 % descended below 980 hPa. However, 9 % of the radiosondes lacked a measured descending branch due to early contact loss. This issue was especially evident during the early phase of the ORCESTRA campaign at INMG on Sal Island, where overlapping transmission frequencies led to radiosondes losing contact earlier than expected. Table 2 provides additional information on ascent and descent statistics, start and end dates, radiosonde vendors, and frequency settings.

Figure 2 shows that radiosonde operations were sustained throughout the ORCESTRA campaign, with activity varying between platforms. The R/V *Meteor* maintained the highest launch frequency, while BCO and INMG operated at lower but also consistent rates.

2.1 INMG

A total of 156 radiosondes were launched at the INMG platform, located at 16.73° N, 22.94° W, 124 of which success-

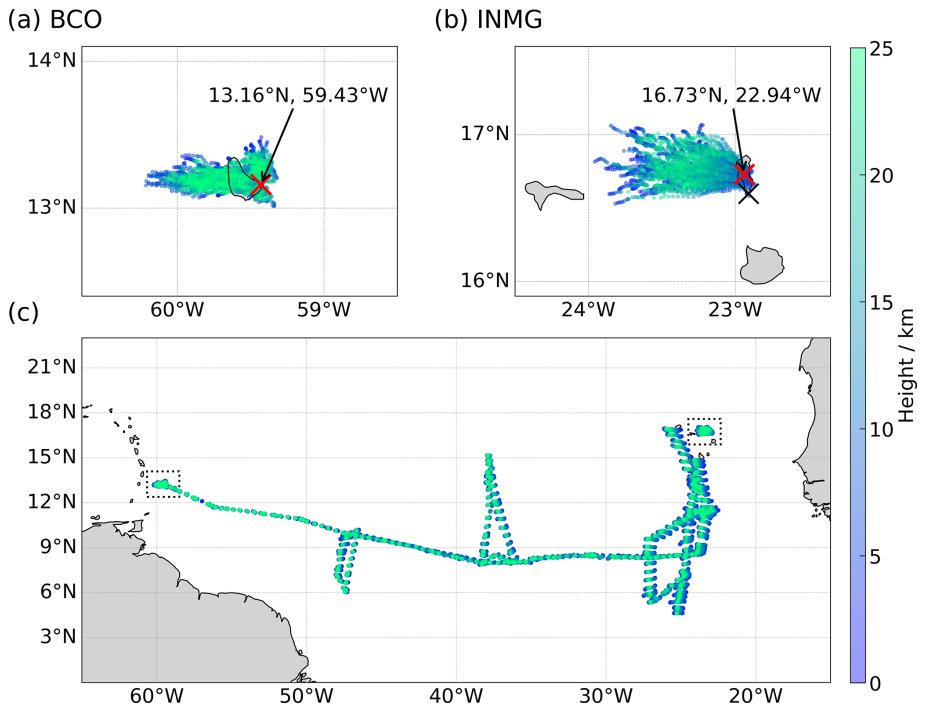

Figure 1. Radiosonde trajectories across the tropical North Atlantic, showing both the ascent and the post-burst descent segments of each balloon-launched radiosonde flight. Each dot marks a location where the radiosonde passed during its flight, color-coded by height. Panels **(a)** and **(b)** show profiles launched from land-based platforms at the Barbados Cloud Observatory (BCO, Deebles Point, Barbados) and Sal Island (INMG, Cape Verde), respectively. The red crosses mark the nominal launch locations, while the black cross in panel **(b)** indicates two soundings launched from a slightly different position at INMG. Panel **(c)** ows all soundings, including those from the R/V *Meteor* during its meridional trajectory across the Atlantic.

Table 2. Launch platform statistics and characteristics. For Meteomodem M20 radiosondes, Eoscan v1.9.221025 was used during the field campaign, while v2.1.241218 was used for post-campaign reprocessing.

	INMG	R/V *Meteor*	BCO
Number of ascents	156	327	141
Number of descents	124	313	135
Start date	9 Aug 2024	14 Aug 2024	7 Sep 2024
End date	11 Sep 2024	24 Sep 2024	29 Sep 2024
Platform altitude/m	58	5.5	17
Frequency/MHz	401.2, 403, 403.6, 404, 404.4	403, 405	400.5–401.5
Balloon type	Hwoyee 200 g	TOTEX TA200-No.088 parachute	TOTEX TA200-No.088 parachute
Radiosonde vendor	Meteomodem	Vaisala	Vaisala
Radiosonde model	M20	RS41-SGP/RS41-SGPe	RS41-SGP/RS41-SGPe
Radiosonde weight/g	36	113	113
Sounding software	Eoscan (v1.9.221025/v2.1.241218)	MW41 (v2.21.0.7)	MW41 (v2.21.0.7)

fully recorded descents. The radiosondes were prepared indoor, where the air temperature was maintained at approximately 25 °C. Initialization and calibration were performed using surface weather conditions measured by the INMG instruments (https://oscar.wmo.int/surface/index.html#/search/station/stationReportDetails/0-20000-0-08594, last access: 9 March 2026).

The balloons were inflated in a nearby hangar where helium was stored. The setup (Fig. 3a) included a net-covered frame to protect the balloon skin and a water bottle used as a weight for accurate filling of the balloon. Radiosondes (Meteomodem, M20) were attached with an unwinder and rope before launch (Fig. 3b). Despite proximity to an airport, no coordination with air traffic control was required.

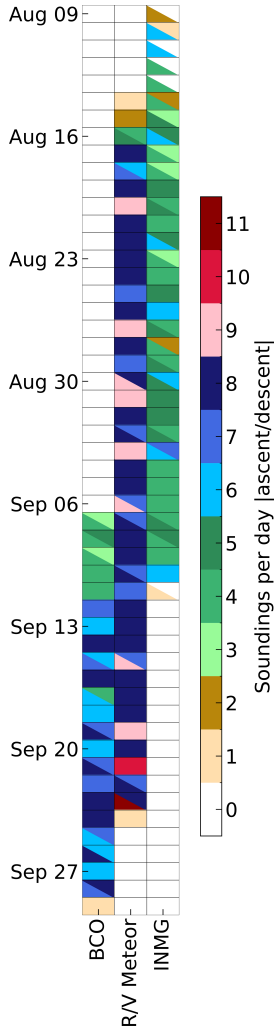

Figure 2. Daily number of ascending (lower left triangles) and descending (upper right triangles) soundings during the 52 d ORCESTRA campaign. The color scale indicates the number of radiosondes per day operated at each platform. Instances where more descents than ascents are recorded (e.g., the second-to-last day at BCO) occur when a radiosonde launched before midnight UTC descends after midnight, shifting the descent count to the next day. The R/V *Meteor*'s dual receiver setup allowed for a higher launch frequency.

During the first 5 d, many radiosondes were lost below 10 km due to interference from a nearby antenna operating on the same frequencies. Consequently, from 9 to 13 August, radiosonde launches were conducted only four times 1 d until a solution was implemented. After the interfering antenna was deactivated, subsequent radiosonde ascents and descents proceeded without issue. However, the limited supply of helium restricted the number of launches, averaging to four per day on non-flight days and six per day on flight days, when either the German research aircraft HALO (https://halo-research.de, last access: 9 March 2026) or the French research aircraft ATR (https://www.safire.fr, last access: 9 March 2026) were conducting measurement flights as part of the PERCUSION or MAESTRO campaign. During this period of interference, two test launches were conducted from alternative nearby locations, resulting in slight deviations from the nominal launch position indicated in Fig. 1b by the black crosses.

Figure 1b shows the trajectories of radiosondes launched from INMG, which predominantly drift westwards under the influence of the easterly trade winds, reaching heights of up to 27.4 km. On average, ascending radiosondes remained airborne for about 110 min and travelled a median distance of 45.7 km, while the descending radiosondes lasted around 28 min with a median drift of 12.4 km.

Radiosonde data from INMG were not distributed to the Global Telecommunication System (GTS) in real time during the campaign. After the campaign and following quality control, the Meteomodem soundings launched from INMG were converted to BUFR format and transmitted in delayed mode to ECMWF for consideration in the ECMWF Reanalysis Version 6 (ERA6) reanalysis.

2.2 R/V *Meteor*

The Research Vessel (R/V) *Meteor* departed from the port of Mindelo on São Vicente Island, Cape Verde, on 16 August and arrived in Bridgetown, Barbados, on 24 September after spending 40 d at sea. Six radiosondes were launched while still in harbor prior to departure on 16 August. In addition to generally steaming westward, the Meteor also performed north/south transects in the eastern, central, and western parts of the tropical Atlantic. During the campaign, a total of 327 radiosondes were launched from the R/V *Meteor*, with 318 successful descents recorded. The radiosondes were prepared and placed in an automatic launcher, with initialization and calibration performed using surface weather conditions measured by the ship's onboard instruments. This was done inside an air-conditioned container except for a few launches when the air conditioning was off in order to troubleshoot condensation build-up. Two ground receivers were used during the campaign: one provided by the Max-Planck-Institut für Meteorologie (MPI) and the other by the German Weather Service (Deutscher Wetterdienst, DWD). For both receiver systems, the radiosondes were briefly taken outside the container to establish a satellite telemetry connection. The difference between the two systems concerned the initialization procedure prior to this step. Radiosondes launched using the MPI receiver (for the 03:00, 09:00, 15:00, and 21:00 UTC ascents) were first initialized indoors using a tray-like adapter connected to the ground station, after which they were taken briefly outside to acquire the satellite signal. In contrast, radiosondes launched using the DWD receiver (for the 00:00, 06:00, 12:00, and 18:00 UTC ascents) were switched on manually using the power button on the sonde

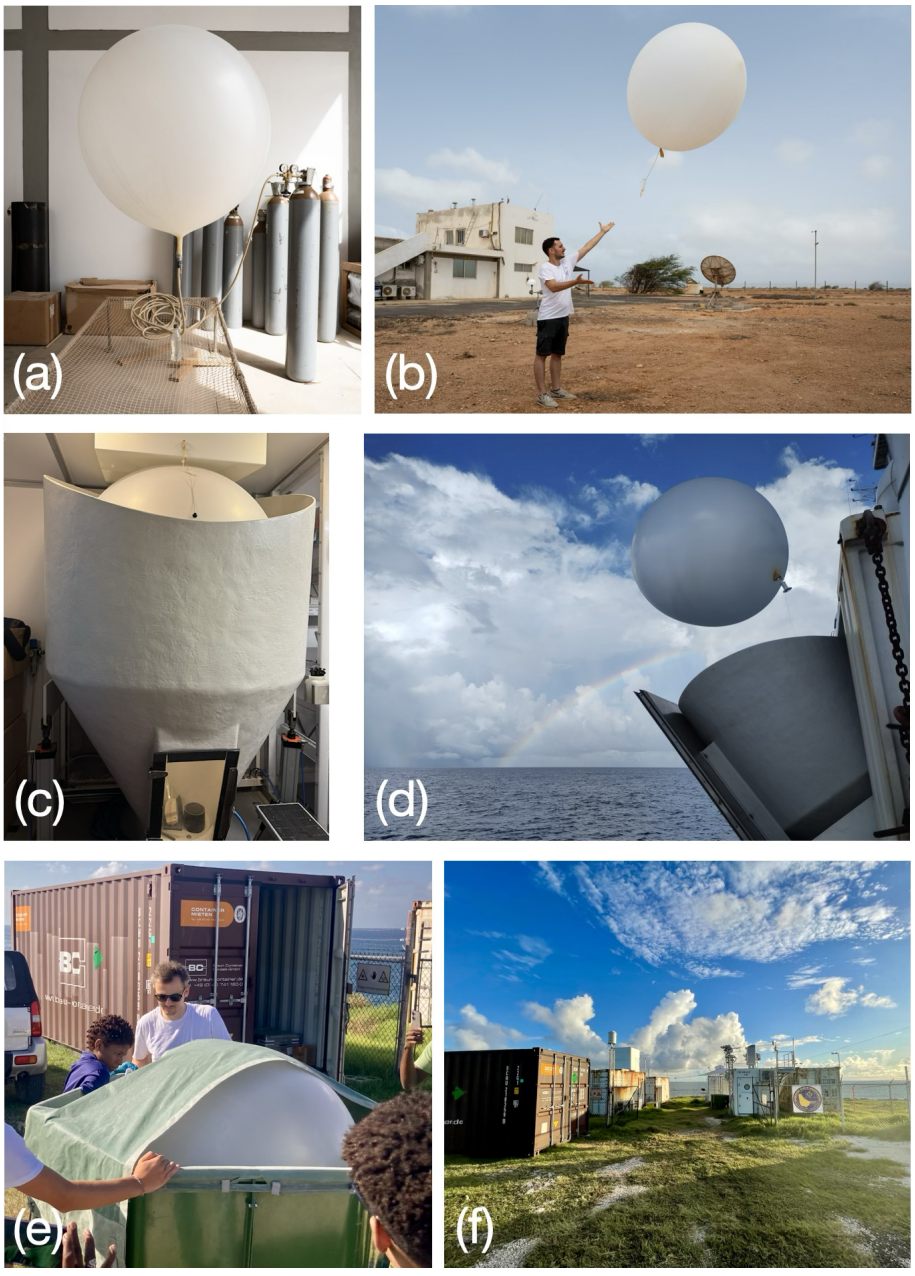

Figure 3. Launching setups on each platform during the ORCESTRA campaign. **(a)** INMG platform on Sal Island, Cape Verde: balloon filling with a water bottle weight and protection from a net-covered frame. **(b)** Radiosonde launch in progress at INMG. **(c)** R/V *Meteor* automatic launcher with ceiling-hung ball for target balloon size. **(d)** Launcher opening for balloon release from the port side. **(e)** BCO launcher with green tarpaulin frame for balloon sizing and skin protection. **(f)** Launch position at BCO near the cliff edge. Credits: **(a, b)** Tristan Vostry; **(c, d)** Allison Wing; **(e)** Nina Robbins-Blanch; **(f)** Marius Winkler.

itself and placed outside to complete their initialization and establish the satellite connection.

The temporarily installed MPI system on board R/V *Meteor* was cross-checked against the permanently installed DWD system to ensure consistency. Height measurements used for radiosonde initialization were taken from the same shipboard instrumentation in both systems. Data integrity immediately after launch was routinely monitored, with each ascent observed for at least 10 min to ensure stable telemetry, correct launch detection, and continuous data reception.

Balloons were prepared inside the automatic launcher and filled with Helium, with each balloon inflated until it touched a ball-shaped control element hanging from the ceiling on a string as shown in Fig. 3c. After successful initialization (as

described above), all radiosondes were brought back inside the container for balloon and unwinder attachment. Figure 3c shows a balloon ready for launch with its radiosonde in the automatic launcher. At the designated launch time, a person had to release a valve to open the launcher, releasing the radiosonde from the port side of the ship. Figure 3d illustrates the open launcher as a radiosonde is launched. During the R/V *Meteor* deployment, radiosondes were launched every three hours, facilitated by the setup of two Vaisala receivers. Additional radiosondes were occasionally launched between the regular times to coincide with EarthCARE overpasses or flights by the High Altitude and Long Range Research Aircraft (HALO).

Figure 1c shows the launch locations of all radiosondes released from the R/V *Meteor*. The color transitions indicate that the radiosondes drifted farther in the eastern than in the western Atlantic. The highest height reached was 28.0 km, corresponding to a pressure as low as 16.0 hPa. On average, ascending radiosondes remained airborne for about 167 min and drifted a median distance of 39.5 km, whereas descending radiosondes lasted around 36 min with a median drift of 10.7 km.

Between 22 September, 20:30 UTC, and 24 September, 03:00 UTC, the R/V *Meteor* was anchored 1.7 km offshore at 13.16° N, 59.41° W, east of the Barbados Cloud Observatory (BCO) at 13.16° N, 59.43° W (Fig. 4a). This allowed for side-by-side comparisons of overland and overwater soundings. During this period, 10 radiosondes were launched simultaneously from both platforms. A similar comparison in the eastern Atlantic was not pursued, as the vessel did not approach the INMG site with comparable spatial proximity. The average surface wind direction was similar at the two platforms, east-northeast (87.7°) at BCO and east-southeast (91.4°) at the R/V *Meteor*, indicating a nearly identical flow regime. The mean profiles in Fig. 4b and their absolute differences in Fig. 4c show very close agreement in both temperature and dew point, with temperature differences remaining well below 1 K. These results support earlier findings (Stevens et al., 2016) that conditions at BCO closely represent those over the adjacent ocean.

Regarding data dissemination, soundings launched at 00:00, 06:00, 12:00, and 18:00 UTC using the permanent DWD receiver were disseminated to the Global Telecommunication System (GTS) as Surface Synoptic Observation (SYNOP) and Upper-Air Temperature (TEMP) messages under the ship identifiers DBBH (until 9 September 2024) and GNJ7EFP (from 10 September 2024), with TEMP data additionally distributed under the identifier ZVQEQCM. These observations were received and processed by the European Centre for Medium-Range Weather Forecasts (ECMWF). In contrast, soundings launched at 03:00, 09:00, 15:00, and 21:00 UTC using the MPI receiver were not transmitted to the GTS, as automatic GTS dissemination was not enabled for this system during the campaign.

2.2.1 Oscillatory radiosonde ascent during rain events

In five cases illustrated in Fig. 5, radiosondes launched from the R/V *Meteor* during rain events displayed pronounced oscillatory behavior. The first ascent phase ended for four of five cases near the freezing level, around 5000 m, after which the radiosonde descended below this altitude before rising again. This ascent–descent cycle repeated several times before the radiosonde ultimately crossed the freezing level and continued to burst altitude. One exception occurred on 11 September 2024, at 07:50 UTC, when the initial ascent extended well above the freezing level. The rain rates taken by a disdrometer[1] aboard the R/V *Meteor* associated with these launches (Fig. 5) place all events within the upper third of rainfall intensities measured during the ship deployment, with some among the most intense observed.

One hypothesis is that the balloon became sufficiently moistened during ascent (indicated by the colorbar in Fig. 5), allowing ice and snow to form and accumulate on its surface near the freezing point. The added weight of accumulated ice and snow may have temporarily halted the balloon's ascent. As the balloon descended into warmer altitudes, the ice and snow likely melted and ran off, allowing the ascent to resume. Such oscillatory behavior of radiosondes has been reported earlier. Venkiteshwaran (1952) used a radiosonde type with a fan indicating vertical motion of the balloon relative to that of the air. Based on this data it was concluded that two types of cases were observed, some where the descent was presumably due to snow accumulated on the balloon, and others where the descent may have been caused by strong subsidence.

2.3 BCO

On 7 September, the first radiosonde was launched from the Barbados Cloud Observatory (BCO, Stevens et al., 2016), located at 13.16° N, 59.43° W. By 29 September, a total of 141 radiosondes were launched, with 135 successful descents recorded. The radiosondes were prepared inside an insulated container, where the air temperature was maintained at approximately 25 °C. Initialization and calibration were conducted using surface weather conditions measured by the BCO instruments. Radiosonde data were not transmitted to the GTS during the ORCESTRA campaign.

The balloons were filled outdoors at the platform with Helium using a radiosonde launcher. Figure 3e shows the setup used for this purpose. The radiosonde launcher, positioned in front of BCO to maintain a safe distance from its measuring instruments and fencing (Fig. 3f), was covered with a fine cloth to protect the balloon skin and equipped with a holding device for safe handling, even in windy conditions. Each balloon was inflated until it nearly touched the

[1] Data found at IPFS CID: bafybeihjcwsecgpmsjxoo5peqafnuqfnalu3ya3vtibwl7qkm76izsnuei.

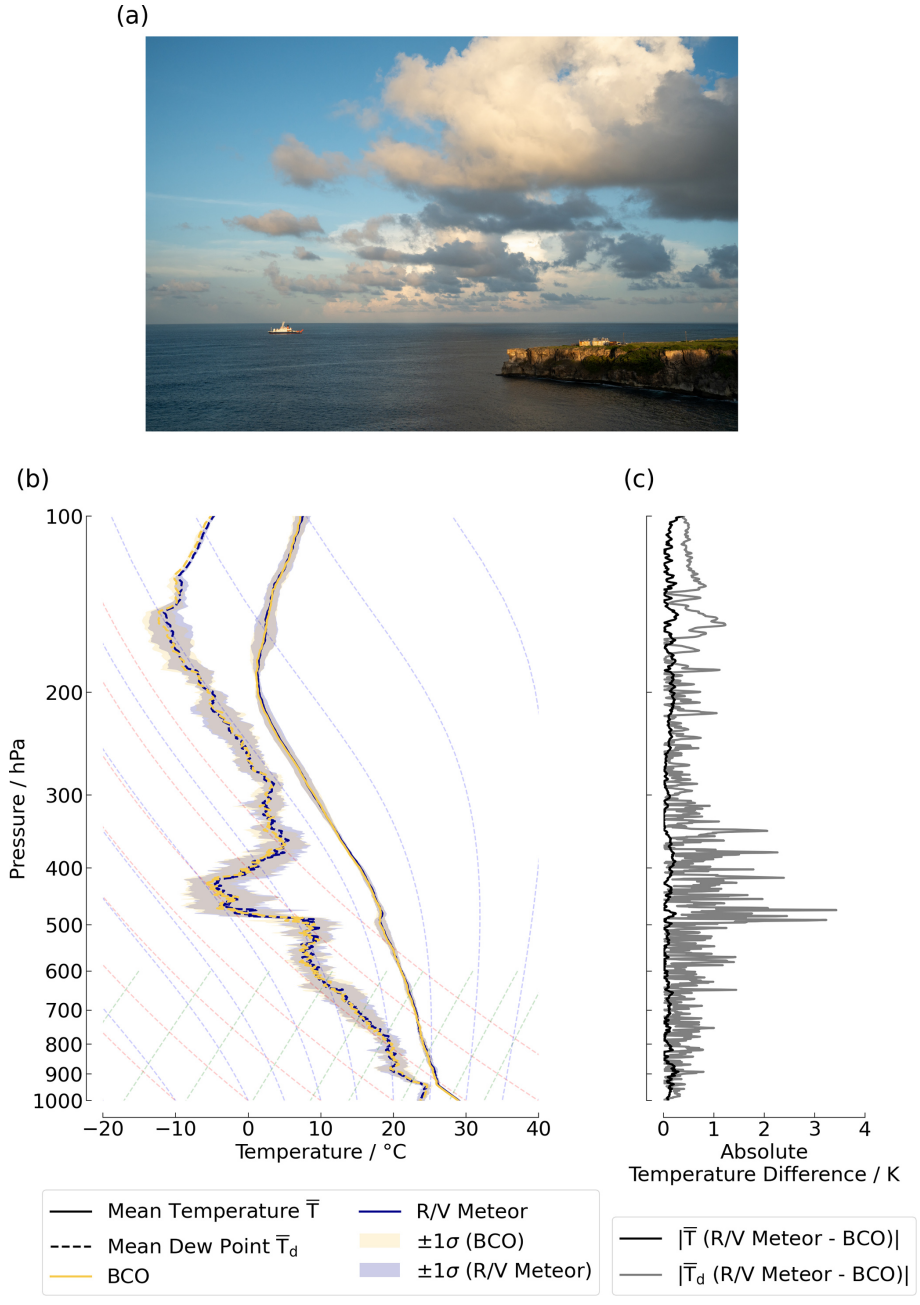

Figure 4. Comparison of the 10 radiosondes that were coordinated between the BCO and the R/V *Meteor*. **(a)** View of the two platforms from Ragged Point Lighthouse (photo credit: Tristan Vostry). **(b)** Mean Skew-T log-P diagram of the paired soundings. **(c)** Corresponding absolute differences in temperature and dew point.

walls of the launcher. A preconfigured radiosonde (Vaisala) fitted with an unwinder was attached to the balloon inside the launcher. At launch time, the balloon was extracted from the radiosonde launcher and released by hand. During the first 5 d of the BCO ORCESTRA campaign, four radiosondes were launched daily at six-hour intervals. Once the helium supply was secured, the schedule increased to eight radiosondes every three hours on flight days (00:00, 03:00, 06:00, 09:00, 12:00, 15:00, 18:00, 21:00 UTC) and six every three hours on non-flight days, excluding the 09:00 and 21:00 UTC slots. On the flight days, the higher launch frequency was timed to coincide with the aircraft operations and to enhance the value of joint measurements.

Apart from telemetry loss of six radiosondes, no technical issues were encountered during the radiosonde mission at the BCO. Variations in launch times were due to the requirement

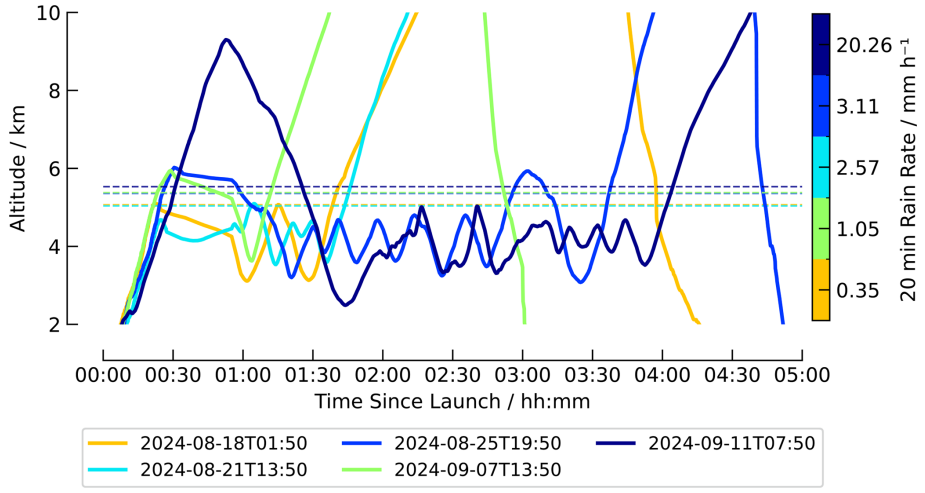

Figure 5. Five radiosondes launched during rain events from the R/V *Meteor* (Vaisala) exhibited oscillatory motion near their respective freezing levels (dashed lines). Rain rates, averaged over the 20 min following launch, are shown by the color bar. Measurements were taken by a disdrometer aboard the R/V *Meteor* and represent conditions at the ship, not along the radiosonde trajectories. The highest rain rate is within the top 2 % of all rainfall recorded during the ship campaign, while even the lowest (yellow) lies within the top 30 %.

of obtaining permission from air traffic control at Grantley Adams International Airport, Bridgetown, Barbados for each launch, ensuring no interference with air traffic. As a result, waiting times of up to 30 min were occasionally necessary.

Figure 1a shows trajectory of the radiosonde launched from BCO, with colors indicating height. The radiosondes reached heights of up to 28.6 km, corresponding to pressures as low as 14.7 hPa. On average, ascending radiosondes remained airborne for about 174 min and drifted a median distance of 24.2 km, while the descending radiosondes lasted around 36 min with a median drift of 8.3 km.

3 Data acquisition

All radiosondes used during the ORCESTRA campaign, whether launched from INMG on Sal Island, the R/V *Meteor*, or the Barbados Cloud Observatory (BCO), shared several core features. Each radiosonde consisted of a transmitter and battery encased in a protective housing, typically made of styrofoam, and included an external sensor boom to measure temperature and humidity. Humidity sensors were equipped with integrated heating to mitigate the risk of icing. By design, these sensors measure relative humidity with respect to liquid water, even at freezing temperatures. In addition, all radiosondes carried a Global Positioning System (GPS) receiver, from which horizontal winds were derived. For Vaisala RS41 sondes, the vertical position is available both as a GPS-based altitude referenced to the WGS84 ellipsoid and as a PTU-based height derived from the pressure sensor. In contrast, Meteomodem M20 sondes determine pressure from altitude and thus provide only GPS-based altitude.

At INMG, radiosondes of type M20 from Meteomodem were used (Meteomodem, 2023) which descend without a parachute. For the radiosonde operations at the R/V *Meteor* and BCO, systems from Vaisala (RS41-SGP; Vaisala Oyj, 2023 and RS41-SGPe; Vaisala Oyj, 2024) were deployed, each equipped with a parachute. The only difference between the two Vaisala models lies in the sensor housing material: the SGP uses styrofoam, while the SGPe employs a biodegradable alternative. The sensors themselves are identical between the two types.

To sample the diurnal cycle of the tropical atmosphere, launches were scheduled so balloons would reach the top of the troposphere near synoptic and intermediate hours (00:00, 03:00, 06:00, 09:00, 12:00, 15:00, 18:00, 21:00 UTC). As shown in Fig. 6, most launches occurred 70–80 min before these target hours. INMG initially operated on an irregular schedule (05:30, 11:30, 14:30, 17:30, 23:30 UTC), but from August 14 shifted to earlier times (04:30, 10:00, 13:30, 16:30, 19:30, 22:30 UTC) to align with data assimilation windows. Although the data were not ultimately assimilated into French NWP models, they were archived for ECMWF Reanalysis Version 6 (ERA6). Variability in INMG launch times also reflected frequent technical issues and relaunches. The R/V *Meteor*'s dual receiver setup enabled flexible, adaptive launches, including those timed to satellite or airplane overpasses. At BCO, coordination with air traffic control sometimes caused delays relative to the planned schedule.

Figure 7 compares ascent and descent rates for Meteomodem and Vaisala radiosondes. Mean ascent rates (Fig. 7a and c) are stable at around 5 m s^{-1} for both types, with a spread of approximately 1 m s^{-1} for Vaisala and 1.5 m s^{-1} for Meteomodem. After balloon burst, mean descent rates in free fall reach up to 30 m s^{-1}, with a spread of about 20 m s^{-1} in the upper atmosphere and less than 5 m s^{-1} near the surface. A weak inflection in the mean descent rate is apparent

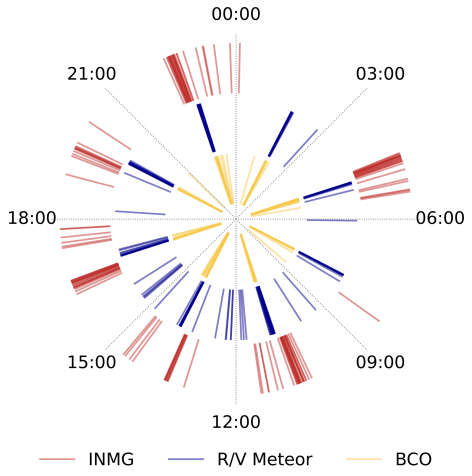

Figure 6. Radiosonde launch times plotted on a 24 h clock. Each radial tick marks a launch, color-coded by platform, with radial distance offset by platform to reduce overlap. Target launch times correspond to standard synoptic and intermediate hours (00:00, 03:00, 06:00, 09:00, 12:00, 15:00, 18:00, 21:00 UTC). Most launches occurred 70–80 min beforehand to ensure the balloon reached the top of the troposphere near the target hour. Deviations arose from air traffic control restrictions at BCO, adaptive timing aboard the R/V *Meteor*, and evolving scheduling and technical issues at INMG.

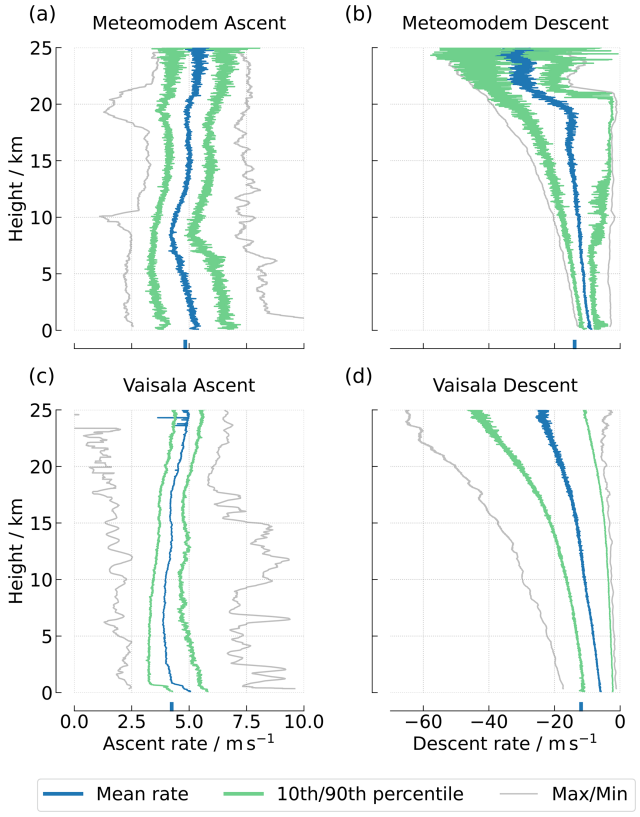

Figure 7. Ascent and descent rates of all radiosondes by vendor. Mean values are shown along with the 10th and 90th percentiles and the maximum and minimum rates at each height level. Bold ticks on the x axes indicate the mean ascent and descent rates below 25 km. The lowest 100 m are omitted because of surface noise.

around 20 km for the Meteomodem sondes (Fig. 7b), near the tropical tropopause in the eastern Atlantic. This feature is not observed for the Vaisala sondes and occurs preferentially over Sal, where the tropopause is more sharply defined and the stronger vertical temperature gradient likely enhances the dynamical response of descending Meteomodem sondes when crossing this layer. Below 15 km, average ascent and descent rates are 4.7 and $-12.8\,\mathrm{m\,s^{-1}}$ for Meteomodem, and 4.1 and $-10.6\,\mathrm{m\,s^{-1}}$ for Vaisala. The higher mean descent rates of Meteomodem sondes reflect their lack of a parachute, while the most extreme descent values, seen in Vaisala sondes, likely result from parachutes that failed or only partially opened, increasing effective weight and descent speed (Ingleby et al., 2022). These ascent and descent characteristics are relevant because they determine the temporal resolution of vertical profiles and can influence measurement uncertainty, particularly during descent when conditions for the sensors are less stable.

Finally, Fig. 8 shows the mean difference between variables measured during descent and those measured during ascent by the same radiosonde. For Vaisala, the MW41 software introduces a descent-phase height bias (Mourad Hamouche, Vaisala Oyj, personal communication, 2025), so heights were recomputed from GPS altitude by removing the local geoid offset and converting to geopotential height. Ascent and descent segments were identified using the radiosonde burst (dropping) flag rather than by altitude. Each sounding was then separated into ascent and descent, pooled, and binned onto a common 10 m grid before calculating mean differences. Meteomodem data were processed directly using GPS altitude from the Level-1 data, which is unaffected by this issue. Pressure values (Fig. 8a) are slightly higher during descent than ascent, with a negligible mean difference of about 12 Pa. Air temperature (Fig. 8b) is marginally higher during descent above 15 km and slightly lower during ascent below this height, with mean differences remaining under 0.5 K. A reversed pattern is observed for relative humidity (Fig. 8c), with overall mean differences below 0.1 %. The question-mark shape seen for Meteomodem results from sensor time lags that become more pronounced during the faster descent and in very low temperatures near the tropopause. The wind speed (Fig. 8d) tends to be higher during ascent than descent, with differences of less than $1\,\mathrm{m\,s^{-1}}$.

To document the processing chain from the raw vendor output to the consolidated campaign dataset, we structure the following description into three stages. First, we describe the Level-0 data, which are the raw radiosonde measurements as delivered by the vendor software. Next, we outline the Level-1 processing, where `PySonde` is used to harmonize the files, separate ascent and descent, and derive additional thermo-

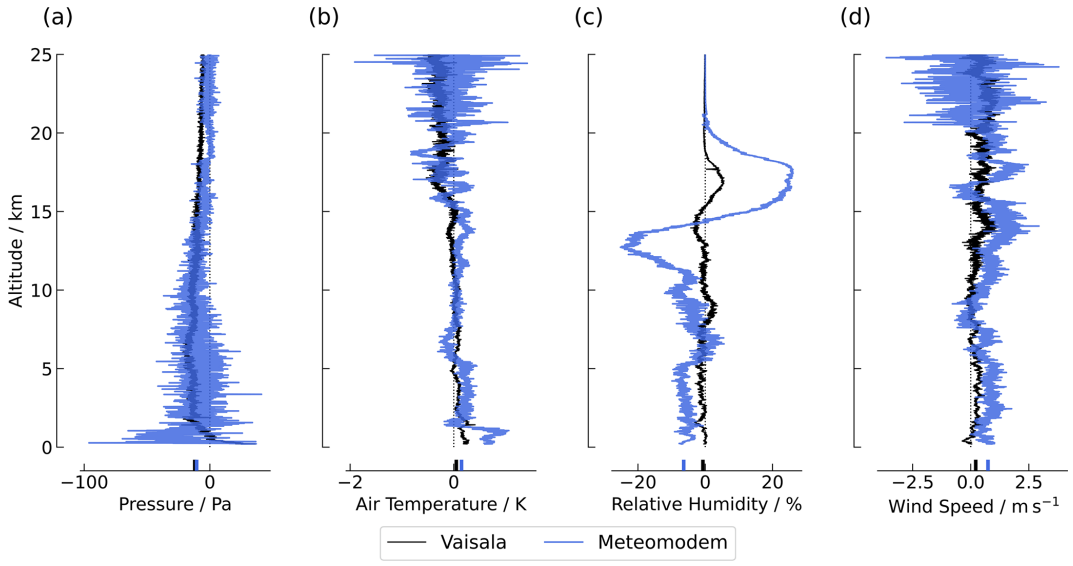

Figure 8. Mean ascent–descent differences by radiosonde type. Profiles show the average ascent minus descent values from the same radiosonde for **(a)** pressure, **(b)** air temperature, **(c)** lative humidity, and **(d)** wind speed. Vaisala is plotted versus geopotential height derived from GPS altitude to avoid the MW41 descent-phase height bias; Meteomodem is plotted versus the dataset's GPS altitude. All variables are pooled across soundings and binned to 10 m before differencing. Bold ticks on the x axis mark the mean ascent–descent difference between 0.2 and 15 km for each type.

dynamic variables. Finally, we present the Level-2 dataset, in which mainly the individual profiles are combined and binned onto a common vertical grid.

3.1 Level-0

The data collected by the radiosondes is transmitted every second to the ground station, where vendor-provided software (Meteomodem Eoscan Software and Vaisala Sounding System MW41) processes the incoming signal and applies an initial quality control prior to any further processing. Both systems detect transmission errors, apply plausibility checks, and record missing or interpolated values with placeholder values. Surface reference measurements obtained immediately prior to launch either from the ground-based meteorological stations (BCO and INMG) or from the ship's onboard instrumentation are incorporated into the output files as the first level of the raw profile.

For Vaisala RS41 radiosondes, this process begins with a mandatory ground check prior to launch. The factory calibration is restored, humidity sensors are reconditioned and subjected to a zero-humidity check, and a built-in temperature check detects damaged units before flight. Pressure sensors are calibrated against a barometer module in the ground check device. During flight, the MW41 software continuously monitors pressure, temperature, humidity, and wind components (zonal, meridional, and absolute). Horizontal winds and positions are derived from GPS signals, while vertical position is available either from a pressure sensor or from GPS-derived altitude, referenced to the WGS84 ellipsoid (Vaisala, 2013).

For Meteomodem M20 radiosondes, the vendor software performs comparable pre-flight checks, verifying sensor performance against surface reference values, restoring calibration, and reconditioning humidity sensors. In flight, the software applies plausibility checks and manufacturer-specific humidity corrections (Dupont et al., 2020), including adjustments for sensor lag and temperature-dependent response. Pressure is primarily determined from GPS altitude. The M20 radiosonde includes an onboard barometric pressure sensor, which is used for launch detection and during the initial phase of the ascent (approximately the first 1000 m). Above this level, pressure is derived from GPS altitude.

The resulting vendor "raw" data, having passed the mentioned vendor's preliminary tests, constitutes the Level-0 product. The Meteomodem software generates files in `.gps` format, which are subsequently processed into `.cor` files, while Vaisala's MW41 software produces `.mwx` files, which are compressed directories containing plain-text `.xml` files with the measured variables. These outputs provide the highest-resolution record of the radiosonde transmission and serve as the starting point for Level-1 processing. An overview of the variables, processing steps, and quality control across all levels is summarized in Table 3.

3.1.1 Quality control at Level-0

In both systems, the vendor software provides the first layer of quality control (QC) by flagging or removing implausible

Table 3. Summary of processing levels, variables, and quality control applied to the ORCESTRA radiosonde datasets. Variable abbreviations are defined as follows: p = pressure; ta = air temperature; RH = relative humidity; dp = dew-point temperature; mr = water vapor mixing ratio; dz = vertical velocity; alt = geometric altitude above the WGS84 ellipsoid; height = geopotential height; wspd = wind speed; wdir = wind direction; θ = potential temperature; q = specific humidity; u, v = zonal and meridional wind components; iwv = integrated water vapor.

Level	Variables contained	Processing steps	Quality Control (QC)
Level-0	*Data variables*: pressure, temperature, relative humidity, wind speed and direction, horizontal and vertical position, and metadata.	Data transmitted every second to ground station; vendor software (MW41/Eoscan) writes raw files (`.mwx` for Vaisala, `.cor` for Meteomodem). Minimal vendor pre-processing: ground check, calibration restore, humidity reconditioning, burst detection.	Vendor QC: transmission error detection, plausibility checks, basic temperature and humidity correction (including radiation error adjustment), flagging with placeholders.
Level-1	*Dimensions*: `sonde_id` × `level`. *Coordinates*: lat (° N), lon (° E), flight_time (UTC), launch_time (UTC), level, sonde_id. *Data variables*: alt (m), p (Pa), ta (K), RH (1), dp (K), mr (1), dz (m s^{-1}; ascent/descent rate), height (m), wspd (m s^{-1}), wdir (deg), platform (label), launch_lat (° N), launch_lon (° E).	Level-0 parsed and harmonized with `PySonde`; placeholders converted to NaN; units/standard_names set; profiles split into ascent/descent (one NetCDF file per branch); derived variables computed: dp, mr, dz; GPS altitude always used for alt, PTU height retrieved from Vaisala `.mwx` files and computed for Meteomodem `.cor` files.	Structural checks (monotonicity of altitude within each branch, duplicate levels removed); physically impossible vendor values already masked as NaN; non-monotonic sections retained but flagged in metadata.
Level-1 (oscillating radiosondes)	*Dimensions*: `sonde_id` × `sample`. *Coordinates*: lat (° N), lon (° E), flight_time (UTC), release_time (UTC), sample, sonde_id. *Data variables*: p (Pa), alt (m), ta (K), RH (1), dp (K), mr (1), dz (m s^{-1}), wspd (m s^{-1}), wdir (deg), platform (label), launch_lat (° N), launch_lon (° E).	Raw `.xml` files inside `.mwx` archives parsed directly, bypassing MW41 burst-cropping. No ascent/descent split; whole oscillatory trajectory kept in one profile. All five oscillating soundings concatenated into a dedicated Level-1 `.zarr` dataset.	QC restricted to NaN handling and thermodynamic plausibility checks; monotonicity of altitude not applicable. No Level-2 product created due to oscillatory vertical profiles.
Level-2	*Dimensions*: `launch_time` × `height`. *Coordinates*: height (m), interpolated_time (UTC), launch_time (UTC), lat (° N), lon (° E). *Data variables*: all Level-1 variables, plus θ (K), q (kg kg^{-1}), wind components u, v (m s^{-1}), iwv (kg m^{-2}), and launch position metadata.	All profiles concatenated into a campaign-wide dataset; all variables vertically interpolated to a uniform 10 m grid up to 31 km. Interpolation combines linear height and log-pressure schemes, masked by occupancy to preserve data gaps. Stored as `.zarr` dataset.	QC ensures structural consistency: height monotonicity enforced, duplicates removed, interpolated values masked by occupancy to retain data gaps. No smoothing or bias correction applied.

values, correcting for known sensor biases (such as humidity response times), and monitoring data continuity throughout the sounding. This automated QC ensures that Level-0 outputs already meet a baseline reliability before further reprocessing.

3.2 Level-1

We use the `PySonde` package v0.0.7 (Schulz et al., 2024) to restructure the quality-controlled Level-0 files into consistent single-profile ascent and descent datasets, to add derived variables, and to save the Level-1 output in NetCDF format.

An earlier version of this package was employed during the EUREC^{4}A campaign to process radiosonde data (Stephan et al., 2021). We have extended `PySonde` to process `.cor` files, enabling us to create a comparable dataset that facilitates easy comparisons between radiosonde measurements from EUREC^{4}A and ORCESTRA (see Table 3).

In the first step, `PySonde` extracts measured values and their associated units from .cor and .mwx files. Vendor-specific placeholder values for missing data are systematically converted to NaN to ensure consistent handling of gaps across platforms. Next, the radiosonde profile is split into ascending and descending segments based on the balloon burst. For Vaisala data, the MW41 software provides an internal burst flag when it detects a sustained increase in pressure; for Meteomodem data, `PySonde` identifies bursts from the transition in the altitude–time series.

For the Level-1 product, several additional variables are derived. The ascent rate is computed from successive height–time differences. Dew-point temperature is calculated from measured temperature T and relative humidity RH following the empirical Vaisala formulation,

$$T_\mathrm{d} = \frac{2T\Lambda}{T\ln\left(\frac{100}{\mathrm{RH}}\right) + 2\Lambda},$$
$$\Lambda = 15\ln\left(\frac{100}{\mathrm{RH}}\right) - 2(T - 273.15) + 2711.5, \quad (1)$$

where Λ is an empirical function that provides an accurate and computationally efficient inversion of the saturation vapor pressure formulation by Hardy (1998), which is used in the Vaisala MW41 processing chain. This expression should not be interpreted as a general inversion of a Magnus- or Tetens-type relation. The saturation mixing ratio is derived following standard thermodynamics (see below). Launch times are standardized to UTC datetimes and stored as the coordinate `launch_time`, ensuring consistent indexing of soundings across platforms. The resulting data are then structured into NetCDF files, saved separately for the ascending and descending branches. Each file in the Level-1 product contains two dimensions: `launch_time`, indexing the individual radiosonde profile, and `level`, representing the vertical sampling points along each ascent or descent.

The mixing ratio mr is computed via:

$$\mathrm{mr} = \frac{\epsilon \cdot \mathrm{RH} \cdot e_\mathrm{s}}{100p - \mathrm{RH} \cdot e_\mathrm{s}}, \quad (2)$$

with e_s the saturation vapor pressure of water, RH the relative humidity in percent (0–100), p is the atmospheric pressure and $\epsilon = \frac{M_\mathrm{v}}{M_\mathrm{d}}$ is the ratio of the molar mass of water vapor to that of dry air.

We compute the saturation vapor pressure of water e_s according to the IAPWS (International Association for the Properties of Water and Steam) formulation by Wagner and Pruß (2002):

$$e_\mathrm{s}(T) = P_\mathrm{c}\exp\left(\frac{T_\mathrm{c}}{T}\left(a_1 v_\mathrm{t} + a_2 v_\mathrm{t}^{1.5} + a_3 v_\mathrm{t}^{3} + a_4 v_\mathrm{t}^{3.5} + a_5 v_\mathrm{t}^{4} + a_6 v_\mathrm{t}^{7.5}\right)\right) \quad (3)$$

with T the air temperature, T_c the critical temperature of water vapor with $T_\mathrm{c} = 647.096\,\mathrm{K}$, P_c critical pressure of water vapor with $P_\mathrm{c} = 22.064 \times 10^6\,\mathrm{Pa}$, $v_\mathrm{t} = 1 - T\,T_\mathrm{c}^{-1}$ and the empirical coefficients: $a_1 = -7.85951783$, $a_2 = 1.84408259$, $a_3 = -11.7866497$, $a_4 = 22.6807411$, $a_5 = -15.9618719$, $a_6 = 1.80122502$.

We compared several commonly used formulations of the saturation vapor pressure over liquid water, including those by Wagner and Pruß (2002), Hardy (1998), Sonntag (1994), Murphy and Koop (2005), and related empirical formulations, against the IAPWS-97 reference. The Wagner–Pruss, Hardy, Sonntag, and Murphy–Koop formulations all show very close agreement with IAPWS-97 within its formal validity range, with deviations typically well below 1 %. In contrast, simpler Magnus- or Tetens-type approximations (e.g., Bolton, 1980) exhibit substantially larger deviations. Below the formal validity range of IAPWS-97, no definitive reference formulation exists; the clustering of empirical formulations at low temperatures therefore does not imply a systematic bias in the IAPWS-based approach. We conclude that replacing the manufacturer-specific formulations (Hardy for Vaisala and Sonntag for Meteomodem) with the consistent IAPWS-97 formulation does not introduce a meaningful bias in derived humidity-related quantities for this dataset.

3.2.1 Quality control at Level-1

In addition to the vendor checks already applied at Level-0, `PySonde` performs additional quality control. All vendor placeholders are replaced by NaN, and values outside physically reasonable ranges (e.g. negative pressures, relative humidities $> 100\,\%$, or temperatures < 150 and $> 330\,\mathrm{K}$) are masked. This masking step is included as a precautionary consistency check; however, in the dataset used for this study no relative humidity values exceeding 100 % were found, so this step does not affect subsequent binning or averaging. Profiles are checked for monotonicity of height during ascent and descent; non-monotonic sections are retained but flagged, as they imply that ascent rate estimates are not physically meaningful. Duplicate vertical levels are removed to avoid inconsistencies in later binning. The guiding principle of Level-1 QC is therefore to ensure structural consistency and remove physically implausible values, while preserving the original measurement information as completely as possible.

3.2.2 Oscillating radiosondes

As described in Sect. 2.2.1 and shown in Fig. 5, five Vaisala RS41 soundings from R/V *Meteor* exhibited oscillatory mo-

tion during ascent. Because the MW41 software misclassified the first temporary descent as the balloon burst, the Level-0 files were prematurely truncated. To recover the full data, we directly accessed the unprocessed .xml files contained inside the .mwx archives. These .xml files provide the actual raw measurements from Vaisala, meaning that the standard vendor QC pplied at Level-0 was not included here. In contrast to the standard workflow, these trajectories were not split into separate ascent and descent branches, since such a distinction is not meaningful for oscillating profiles. Instead, each trajectory was retained in its entirety as a single file with the dimensions `sounding` × `sample`

From these raw measurements we extracted the standard observed variables and, using individual `PySonde` functions, computed dew point temperature and mixing ratio. The five recovered soundings were merged into a dedicated Level-1 `.zarr` dataset. No Level-2 product was generated for the oscillating radiosondes (see Table 3), as Level-2 processing requires monotonic ascent or descent and subsequent binning onto a uniform vertical grid, conditions not met by these oscillatory profiles.

3.3 Level-2

The Level-2 product builds on the processed Level-1 data (cf. Table 3), which contain the cleaned and derived measurements from individual soundings.

Before vertical interpolation, each Level-1 profile is checked for monotonicity in its height coordinate. For both ascent and descent segments, height is expected to vary consistently in one direction. Duplicate height levels are removed to ensure uniqueness.

Each profile is then vertically interpolated onto a uniform height grid extending from the launch level to 31 km in 10 m increments. The vertical interpolation combines a linear interpolation in height with a dedicated log-pressure interpolation to preserve the physical structure of the $p(z)$ profile. A per-variable occupancy mask, derived from a temporary bin, ensures that interpolated values are retained only where the original profile contained valid data, preventing artificial layers. This two-step approach preserves the vertical integrity of the measurements while maintaining data honesty by leaving gaps where no observations exist in the raw profile.

On this common vertical grid, additional variables are derived, including potential temperature (θ), specific humidity (q), and integrated water vapour (IWV). After interpolation and variable derivation, all processed profiles are concatenated into a combined multi-sounding dataset and stored in Zarr format for distribution via the InterPlanetary File System (IPFS).

We derive potential temperature, specific humidity and IWV as follows. Potential temperature is computed with MetPy as

$$\theta = T\left(\frac{p_0}{p}\right)^{R_\mathrm{d}/c_{\mathrm{p_d}}},\ p_0 = 10^5\,\mathrm{Pa}, \tag{4}$$

where T is air temperature (K), p is pressure (Pa), $R_\mathrm{d} = 287.05\,\mathrm{J\,kg^{-1}\,K^{-1}}$ is the gas constant for dry air, and $c_{\mathrm{p_d}} = 1004.0\,\mathrm{J\,kg^{-1}\,K^{-1}}$ is the specific heat capacity of dry air at constant pressure.

Specific humidity q is obtained from the mixing ratio mr via

$$q = \frac{\mathrm{mr}}{1+\mathrm{mr}}. \tag{5}$$

IWV is computed by vertically integrating the water-vapour mass density over height. For this, realistic values require continuous measurements, particularly in the lower atmosphere where most of the water vapor resides. Profiles with missing data segments would lead to biased or physically meaningless IWV estimates. Therefore, we apply a four-step filtering procedure before solving the following integral (Schulz and Stevens, 2018):

$$\mathrm{IWV} = \int q(z)\rho(z)\mathrm{d}z, \tag{6}$$

where q is the specific humidity and ρ the air density derived from pressure and virtual temperature.

First, we exclude soundings from R/V *Meteor* launched before 16 August, when the vessel was still docked in the port of Mindelo, Cape Verde, and thus did not sample open-ocean conditions. These launches were conducted while the vessel was in port, occurred sporadically rather than following the regular 8-per-day schedule, and were not accompanied by concurrent shipborne measurements. They are therefore excluded only from the IWV analysis to ensure a consistent focus on open-ocean conditions. Including them would introduce a small number of profiles influenced by coastal effects, leading to a slightly drier tail in the IWV distribution that is not representative of the open Atlantic.

Second, we retain soundings that reach at least 8 km height and contain data below this level. The 8 km threshold is a practical cutoff chosen for comparability with HALO dropsonde coverage during PERCUSION, although many dropsonde profiles extend higher.

Third, within the 0–8 km layer we require that no more than 20 % of vertical levels are missing when considering the simultaneous availability of humidity q, pressure p, and temperature T (i.e., a level counts as valid only if all three are finite).

Fourth, we enforce sufficient near-surface sampling by keeping only profiles with at least 50 levels in the lowest 1 km where q, p, and T are all finite.

Small internal gaps are then filled along height using linear interpolation for q and T, and log-linear interpolation for p; endpoints of p and T are extrapolated by forward/backward filling. The Level-2 product used for the IWV computation is obtained by vertically resampling the raw profiles onto a fixed 0–31 km altitude grid. Because the actual

launch altitude differs between platforms and sites (e.g. land stations versus ship deck), the lowest valid measurement in the resampled profile corresponding to the surface reference (ground-station or shipboard) value contained in the raw profile does not necessarily coincide with the 0 m grid level. Consequently, some Level-2 profiles lack a valid near-surface humidity value at the lowest grid levels. To enable a physically meaningful IWV integration, near-surface q is therefore backfilled only up to 300 m to bridge short launch-adjacent gaps; if the first (surface) levels of q remain missing after this limited backfill (e.g., a gap > 300 m), the profile's IWV is masked and excluded from IWV statistics. We do not extrapolate q beyond this limit (only p and T are extrapolated at the ends). In total, 72.1 % of soundings remain available for analysis after filtering.

3.3.1 Quality control at Level-2

Quality control at Level-2 focuses on ensuring structural consistency of the vertical profiles and transparency of the binning procedure. Empty grid points remain explicitly missing rather than filled by interpolation, and duplicate or non-monotonic levels are removed. No additional smoothing or bias correction is applied: the guiding principle of Level-2 QC is to provide a harmonized, intercomparable dataset while preserving the raw variability of individual soundings.

4 Observed atmospheric conditions during ORCESTRA

Figure 9 summarizes the vertical structure of winds, humidity, and moist static energy observed during ORCESTRA. Across all sites, the profiles reveal coherent patterns that reflect the large-scale circulation of the tropical Atlantic rather than local variability. Easterly winds dominate the zonal wind profiles at BCO, INMG, and the R/V *Meteor* west of 40° W, while the R/V *Meteor* east of 40° W records westerlies below 700 hPa that shift to easterlies aloft. In the meridional wind, BCO and the R/V *Meteor* show northerlies below 700 hPa, whereas INMG exhibits southerlies in the lower atmosphere and northerlies above, resulting in a mean net northward flow.

Relative humidity in the boundary layer is highest at INMG and on the R/V *Meteor* east of 40° W, followed by the R/V *Meteor* west of 40° W and BCO. At INMG, humidity decreases sharply just above the surface until about 700 hPa, while at the other platforms the decline with height is more gradual.

Moist static energy (MSE) was computed following $\mathrm{MSE} = c_\mathrm{p}T + L_\mathrm{v}q + gz$, where T is temperature, q specific humidity, and z height. The calculation used the Python package `moist_thermodynamics` by Bjorn Stevens (https://github.com/mpimet/moist_thermodynamics, last access: 9 March 2026), which incorporates composition-dependent heat capacities. Relative humidity was recomputed from radiosonde measurements using temperature-dependent saturation vapor pressures over liquid and ice, based on the IAPWS formulations of Wagner and Pruß (2002) for liquid water and Wagner et al. (2011) for ice. The highest MSE values in the lower atmosphere are observed at BCO, followed by the R/V *Meteor* west of 40° W, R/V *Meteor* east of 40° W, and INMG. Above 700 hPa, MSE from BCO is the smallest, while the R/V *Meteor* east of 40° W shows the slowest decrease with height.

Figure 10 shows the evolution of vertical relative humidity profiles throughout the campaign. The R/V *Meteor*'s early profiles, collected in the eastern Atlantic near Sal (22.56° W), closely resemble those from INMG, while later profiles, taken when the ship was anchored near BCO (59.43° W), match BCO's vertical structure more closely. Relative humidity was recalculated over liquid water for $T > 0$ °C and over ice for $T < 0$ °C. Pronounced mid-tropospheric variability reflects the passage of large-scale synoptic disturbances, including tropical waves, which modulate moisture and convection across the basin. A similar temporal pattern is evident in Fig. 11, which presents the corresponding air temperature anomalies.

Figure 12 shows the IWV for each platform in the campaign for both ascending and descending radiosondes. The R/V *Meteor* sampled the moistest environment, with a mean IWV of 57.6 kg m^{-2}. INMG, situated on Sal Island in the eastern Atlantic, recorded a mean IWV of 51.6 kg m^{-2}. BCO exhibited a bimodal distribution, with peaks near 43 and 57 kg m^{-2}, and a mean of 52.9 kg m^{-2}. These patterns are consistent with the vertical humidity structures shown in Fig. 10.

Descending profiles are more prone to incomplete near-surface coverage and potential sensor hysteresis effects. However, the strict IWV filtering criteria described in Sect. 3.3 ensure physically meaningful column integrals for both ascent and descent segments. An analysis restricted to ascent profiles yields qualitatively similar IWV distributions, with only minor quantitative differences and unchanged relative offsets between platforms. The combined ascent–descent dataset is therefore used to provide the most comprehensive representation of the observed variability.

Table 4 presents a selection of extreme values for each platform, excluding the five oscillating radiosondes launched from R/V *Meteor*. At BCO, the launch reaching the lowest air pressure coincided with the longest recorded horizontal travel distance of 62.1 km. The maximum travel distance of 116.9 km was recorded by a radiosonde launched from R/V *Meteor*, 1 d after the peak wind speed of 42.1 m s^{-1} at 13.5 km. The coldest overall temperature, −85.5 °C, was recorded by a radiosonde launched from INMG on 24 August at 22:33 UTC at 17.5 km.

Figure 13 shows the maximum height reached by each radiosonde per platform as a histogram. The campaign median is 25.1 km indicated by the dashed black line. Radiosondes launched from INMG on Sal Island, Cape Verde, show a

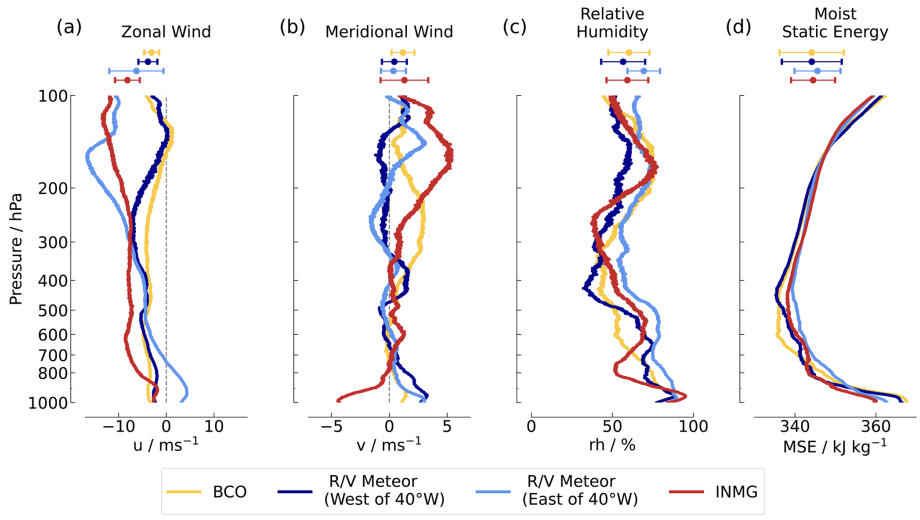

Figure 9. Mean profiles from the entire ORCESTRA campaign, based on radiosonde data from BCO, INMG (Sal Island), and the R/V *Meteor*. Shipboard profiles are split into two regions: east of 40° W and west of 40° W, representing different phases of the Atlantic transect. Panels show **(a)** zonal wind, **(b)** meridional wind, **(c)** relative humidity (computed over liquid above and over ice below freezing temperature), and **(d)** moist static energy as a function of pressure. Profiles are averaged over both ascending and descending soundings. Markers at the top indicate the mean (circle) and one standard deviation (horizontal bars) of the column-averaged values for each platform.

Table 4. Selected extreme values measured by radiosondes at each platform, including UTC timestamps and corresponding heights. The five oscillating radiosondes launched from the R/V *Meteor* are excluded.

	Coldest temperature	max. wind speed	Min. wind distance	Longest height	Highest pressure	Lowest
BCO	−80.8 °C (9 Sep 2024 16:48:39Z at 16.6 km)	29.4 m s^{-1} (12 Sep 2024 22:52:28Z at 26.4 km)	0.0 m s^{-1} (12 Sep 2024 19:49:59Z at 6.5 km)	62.2 km (14 Sep 2024 19:53:38Z)	28.6 km (14 Sep 2024 19:53:38Z)	14.7 hPa (14 Sep 2024 19:53:38Z at 28.5 km)
R/V *Meteor*	−84.9 °C (24 Aug 2024 19:50:05Z at 17.7 km)	42.1 m s^{-1} (24 Aug 2024 10:46:17Z at 13.4 km)	0.0 m s^{-1} (23 Sep 2024 00:39:17Z at 17.2 km)	116.9 km (25 Aug 2024 16:50:16Z)	28.0 km (12 Sep 2024 22:47:02Z)	16.0 hPa (12 Sep 2024 22:47:02Z at 28.0 km)
INMG	−85.5 °C (24 Aug 2024 22:33:52Z at 17.5 km)	32.8 m s^{-1} (22 Aug 2024 20:50:38Z at 20.6 km)	0.0 m s^{-1} (5 Sep 2024 23:49:51Z at 4.8 km)	89.8 km (15 Aug 2024 17:24:59Z)	27.4 km (14 Aug 2024 14:29:08Z)	17.5 hPa (14 Aug 2024 14:29:08Z at 27.3 km)

small peak below 5 km which can be linked to early loss of contact with radiosondes immediately after launch in the beginning of the campaign, caused by an interference signal. While the radiosondes launched from BCO (Vaisala, RS41-SGP&-SGPe) reached highest height values, the majority of all radiosondes launched from R/V *Meteor* (Vaisala, RS41-SGP&-SGPe) climbed further than the campaign median. Radiosondes launched from INMG (Meteomodem) have a tendency to burst before the campaign median.

5 Code and data availability

The raw data output by the respective software of the radiosonde manufacturers Vaisala and Meteomodem after a successful measurement was processed using `PySonde` (v0.0.7) (https://doi.org/10.5281/zenodo.13831915, Schulz et al., 2024), converting Level-0 data to Level-1 and subsequently to Level-2. For five oscillating Vaisala RS41 sondes launched from R/V *Meteor*, the manufacturer's software prematurely truncated the profiles; these were therefore recovered

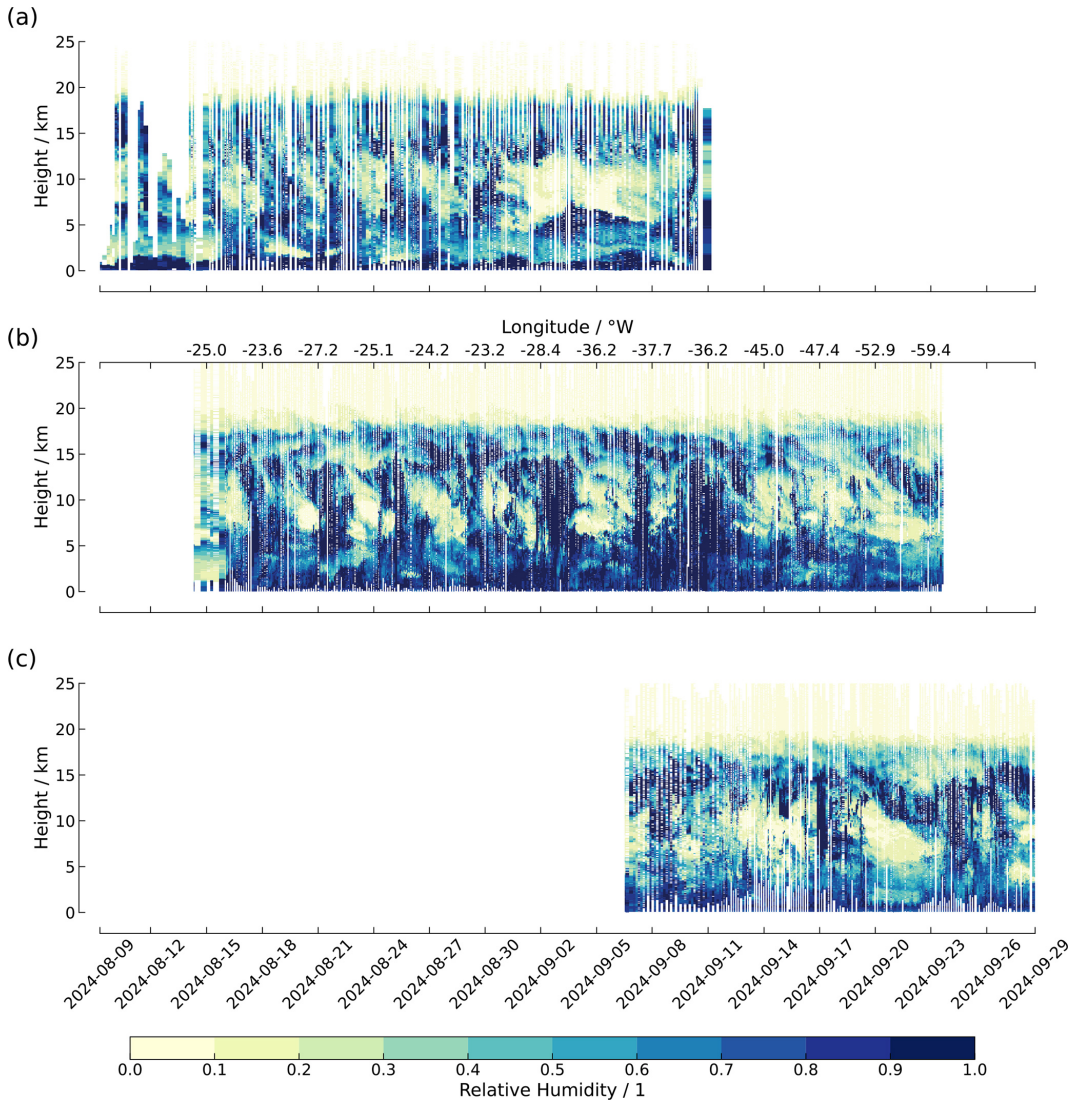

Figure 10. Time–height cross sections of relative humidity from radiosondes launched at **(a)** INMG on Sal Island, **(b)** the R/V *Meteor*, and **(c)** BCO, covering the full campaign period at each platform. In panel **(b)**, a secondary *y* axis at the top shows the ship's longitude as it traversed the tropical Atlantic from east to west.

directly from the unprocessed `.xml` files within the `.mwx` archives.

The resulting datasets are published via the InterPlanetary File System (IPFS) and can be accessed through the ORCESTRA Data Browser (https://browser.orcestra-campaign.org, last access: 9 March 2026), which provides a graphical interface to search, preview, and download the `zarr` dataset collections using a standard web browser. This browser-based access is the recommended entry point for most users and does not require any local installation.

The following datasets were produced as part of this study (Winkler et al., 2025a):

- *RAPSODI Raw Radiosonde Measurements during ORCESTRA (Level 0)*:
  BCO (Winkler et al., 2025b): https://ipfs.io/ipns/latest.orcestra-campaign.org/raw/BCO/radiosondes/ (last access: 9 March 2026)
  INMG (Winkler et al., 2025c): https://ipfs.io/ipns/latest.orcestra-campaign.org/raw/INMG/radiosondes/ (last access: 9 March 2026)
  R/V *Meteor* (Winkler et al., 2025d): https://ipfs.io/ipns/latest.orcestra-campaign.org/raw/METEOR/radiosondes/ (last access: 9 March 2026).

- *RAPSODI Oscillating Radiosonde Measurements during ORCESTRA (Level 1)*:
  DOI: https://doi.org/10.82246/BAFYBEIHXRAJOJUQ (Winkler et al., 2026).

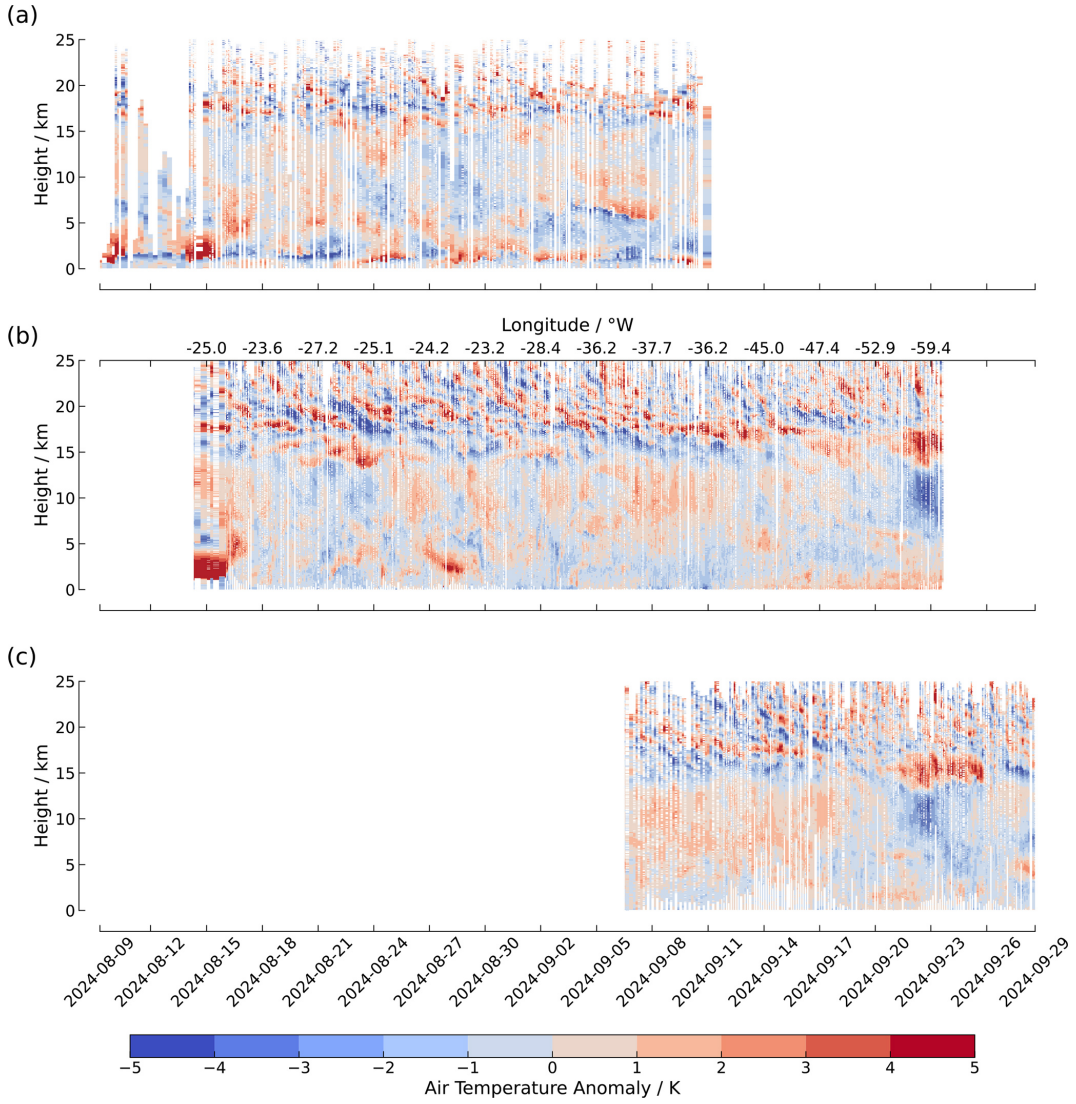

Figure 11. Vertical profiles of air temperature anomalies over time. Panels show time–height cross sections of temperature anomalies from radiosonde soundings launched at **(a)** INMG on Sal Island, **(b)** R/V *Meteor*, and **(c)** BCO. Anomalies were computed separately for each platform by subtracting the mean temperature profile at each altitude level over time. The full set of soundings from each platform is included. Positive anomalies are shown in red, and negative anomalies in blue. Panel **(b)** features a secondary x axis at the top indicating the longitude of the ship as it progressed across the tropical Atlantic.

- *RAPSODI Radiosonde Measurements during ORCESTRA (Level 1) (merged, padded to common vertical levels)*:
  DOI: https://doi.org/10.82246/BAFYBEIA34AUWYV (Winkler and Rixen, 2026a).
- *RAPSODI Radiosonde Measurements during ORCESTRA (Level 2)*:
  DOI: https://doi.org/10.82246/BAFYBEID7CNW62Z (Winkler and Rixen, 2026b).

For users wishing to access the `zarr` datasets programmatically, direct access via IPFS is supported. This requires either a locally running IPFS client or access via a public IPFS gateway. General information on IPFS concepts and installation is available at https://docs.ipfs.tech/ (last access: 9 March 2026).

When using Python, access to the datasets additionally requires the packages `xarray`, `zarr`, `fsspec`, and `ipfsspec`, which can be installed via:

```
pip install xarray zarr fsspec ipfsspec
```

The Python scripts used to generate all figures in this paper are available in a dedicated repository (https://github.com/mariuswinkler/Winkler_et_al_RAPSODI_Data_Paper_2025.git, last access: 9 March 2026). The version of `PySonde` employed for the processing, including campaign-specific configuration files, is archived sepa-

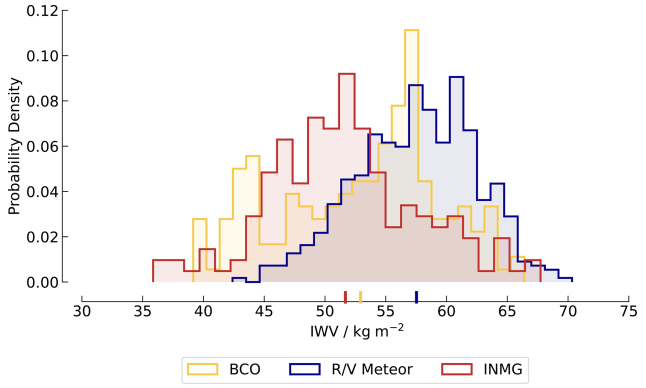

Figure 12. Histograms of integrated water vapor (IWV) from radiosonde launches at BCO, the R/V *Meteor*, and INMG. Bold vertical ticks along the x axis indicate the mean IWV for each platform. Analysis includes 72.1 % of all soundings after filtering.

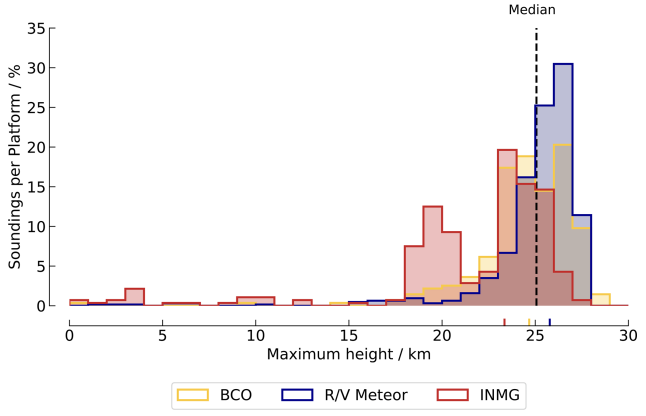

Figure 13. Maximum altitude distribution per platform. Histograms show the maximum altitude reached by radiosondes launched from BCO, R/V *Meteor*, and INMG. Colored x axis ticks indicate the median highest altitude reached at each platform. The vertical dashed line indicates the campaign-wide median altitude of 25.1 km.

rately (https://github.com/mariuswinkler/Winkler_et_al_RAPSODI_PySonde_for_Data_Paper_2025.git, last access: 9 March 2026).

In Python, the data can be accessed directly from IPFS. The following example shows how to load the Level-1 oscillating radiosonde, Level-1 merged (padded to common vertical levels), and Level-2 concatenated datasets:

```
import xarray as xr

RAPSODI_Oscillating = xr.open_dataset(
    "ipfs://bafybeihxrajojuqzyx65qso7ama6ngvreetkdw3hqzx3sdzfb7lcmg6vaq",
    engine="zarr"
)
RAPSODI_Level1 = xr.open_dataset(
    "ipfs://bafybeia34auwyvbh2rq7cn7aguzz7pulq2krdddieesm6kpysirsui7c4m",
    engine="zarr"
)
RAPSODI_Level2 = xr.open_dataset(
    "ipfs://bafyboid7cnw62zmzfgxcvc6q6fa267a7ivk2wcchbmkoyk4kdi5z2yj2w4",
    engine="zarr"
)
```

6 Summary

This paper presents the Radiosonde Atmospheric Profiles from Ship and island platforms during ORCESTRA, collected to Decipher the ITCZ (RAPSODI) – a quality-controlled dataset encompassing all radiosonde profiles conducted during the ORCESTRA campaign. ORCESTRA is a large-scale field study carried out in August and September 2024, with radiosonde observations playing a central role. These observations provide vertical profiles of temperature, humidity, wind, and pressure across the tropical Atlantic, spanning the region between 4 and 17° N, and from 20 to 60° W.

Radiosondes were launched from three platforms strategically distributed across the basin: the National Institute of Meteorology and Geophysics (INMG) on Sal Island, Cape Verde, in the eastern Atlantic; the research vessel R/V *Meteor*, which traversed the Atlantic from east to west; and the Barbados Cloud Observatory (BCO) in the western Atlantic. Over the course of the campaign, a total of 624 radiosondes were launched, most of which returned both ascent and descent measurements. Data quality varied across platforms due to factors such as early loss caused by radio interference and environmental conditions, including humidity and precipitation.

The dataset was processed in three stages. Level-0 comprises the raw data output by the Meteomodem and Vaisala ground station software, which already includes the manufacturer's built-in quality control such as ground checks, calibration restoration, humidity sensor reconditioning, and plausibility filtering during flight. Level-1 data is generated from these files using the `PySonde` package, which restructures the profiles into consistent ascent and descent segments, converts vendor placeholders to missing values, and adds several derived thermodynamic variables. In addition, a dedicated Level-1 dataset was created for five oscillating Vaisala sondes launched from R/V *Meteor*, for which `PySonde` could not be applied. Level-2 builds on the Level-1 product by checking for monotonic ascent or descent, computing further diagnostics, and binning all soundings onto a uniform vertical grid for analysis.

The RAPSODI radiosonde observations enable a broad range of scientific investigations into tropical atmospheric processes, with a focus on the structure and variability of the Atlantic Intertropical Convergence Zone (ITCZ). The dataset provides high-vertical-resolution thermodynamic and wind profiles from repeated launches across an east–west transect spanning ITCZ core, edge, and adjacent subsidence regimes. In combination with the complementary observations collected from aircraft, ship-based, and ground-based remote-sensing platforms during ORCESTRA, this dataset enables studies of tropospheric stability, vertical wind shear, moisture convergence, and the vertical distribution of moist static energy, as well as investigations of boundary-layer processes, convective transitions, cold-pool influences, and the coupling

between clouds, circulation, and radiation. The vertical profiles reflect a gradient in atmospheric moisture: R/V *Meteor* operated predominantly in moist conditions, BCO sampled both moist and dry environments, and INMG remained primarily in drier air throughout the campaign. In particularly moist conditions associated with heavy rainfall, some profiles from R/V *Meteor* exhibited rare oscillatory behavior. The quality-controlled dataset is published in Zarr format on the Inter Planetary File System (IPFS) for public access.

Author contributions. Writing and visualization (original draft) were carried out by MW, with plotting contributions from MR. Writing (review and editing) and dataset validation were performed by MW with feedback from MR, FB, FC, PP, HSeg, HSch, JC, EF, HMG, BP, NRB, DK, RV, SB, AAW, and BS. The responses to the review process and corresponding manuscript revisions were led by MW with feedback from AAW, HSeg, DK, FC, JC and FJ.

MW led the overall data curation, processing, and quality control, and ensured persistent dataset availability through the IPFS. Data curation included adapting the `PySonde` package to campaign needs, with MR implementing the processing of proprietary `.cor` files. KHW developed a method to process oscillating soundings directly from raw `.mwx` files, bypassing the MW41 system limitations. The author list reflects different levels of responsibility and contribution to the radiosonde operations and dataset preparation.

- Group 1 – Mission leads (MW–KHW): MW and MR were responsible for BCO; FB, FC, and PP for INMG; HSeg, HSch, and KHW (together with DK and AAW from Group 3) for R/V *Meteor*. Tasks included ensuring that hardware and software were in place, creating launch schedules, managing shifts, and taking overall responsibility in coordination with the principal investigators (Group 3). CCN contributed to scheduling FSU students who helped launch radiosondes at BCO.
- Group 2 – Launch operations (EAB–CW): (Indicated by a symbol in the author list.) These authors participated in radiosonde shifts and took responsibility for timely launches. Authors in this group are listed alphabetically.
- Group 3 – Strategy (DK–BS): principal investigators who contributed to the design of the overall radiosonde strategy.

Competing interests. The contact author has declared that none of the authors has any competing interests.

Disclaimer. Publisher's note: Copernicus Publications remains neutral with regard to jurisdictional claims made in the text, published maps, institutional affiliations, or any other geographical representation in this paper. The authors bear the ultimate responsibility for providing appropriate place names. Views expressed in the text are those of the authors and do not necessarily reflect the views of the publisher.

Acknowledgements. We thank the staff of the INMG and the Mindelo Ocean Science Center in Cape Verde for their collaboration and operational support. The atmospheric soundings at INMG benefited from access to the National Instrument Moyens Mobiles, which is part of the ACTRIS-FR research infrastructure.

We gratefully acknowledge Lukas Kluft and Tobias Koelling for their support in establishing and maintaining the IPFS infrastructure, and thank Theresa Mieslinger for her constructive internal review.

We thank the two anonymous reviewers for their careful reading of the manuscript and for their constructive comments, which helped to improve the clarity and quality of this paper.

Financial support. Sandrine Bony and many MAESTRO participants (GB, VD, CD, JLD, EF, ELG, ML, NM, BMcK, BP, NR, JT) acknowledge support from the European Research Council (ERC) under the Horizon Europe programe (MAESTRO, grant no. 101098063). Sal radiosoundings were also funded by the MAESTRO ERC grant. Abdou Aziz Coly and Diouf Ousseynou (from ANACIM) acknowledge support from Wedig von Gaudecker and the Luciole Foundation of the French Science Academy.

We are grateful to the Deutscher Wetterdienst (DWD) for providing the second receiver on R/V *Meteor*. Martin Stelzner (DWD) contributed one launch per day as part of the regular operation of the DWD weather station on the ship and provided essential advice on launch procedures at sea. Nearly all members of the BOWTIE science team as well as the crew of Meteor assisted with radiosonde launches, without whom the campaign would not have been possible. Technical support for the installation and deinstallation phases on Meteor was provided by Friedhelm Jansen and Björn Brüggemann.

Funding for R/V *Meteor* cruise M203 was provided by the Deutsche Forschungsgemeinschaft (DFG) under grant number GPF20-1072. Raphaela Vogel and Nina Robbins-Blanch acknowledge support from the European Research Council (ERC) under the Horizon Europe programme (ROTOR, grant no. 101116282). Fleur Couvreux, Florent Beucher, and Philippe Peyrillé acknowledge support from the French National programme LEFE (Les Enveloppes Fluides et l'Environnement) through the ILSOM project. PICCOLO and its participants (MMB, DCB, WTH, SK, MK, TYL, ML, EL, NRM, JHR, JCS, CS, MS, AT, CW, CCN, and AAW) are supported by the US National Science Foundation (NSF) through Awards No. 2331199, 2331200, and 2331202.

At BCO, radiosonde operations and infrastructure were supported by the technical staff Friedhelm Jansen and Björn Brüggemann. Radiosondes at the BCO were in part funded through the CLICCS Cluster of Excellence (EXC 2037, Project 390683824).

The article processing charges for this open-access publication were covered by the Max Planck Society.

Review statement. This paper was edited by Luis Millan and reviewed by two anonymous referees.

References

Bolton, D.: The Computation of Equivalent Potential Temperature, Mon. Weather Rev., 108, 1046–1053, https://doi.org/10.1175/1520-0493(1980)108<1046:TCOEPT>2.0.CO;2, 1980.

Dupont, J.-C., Haeffelin, M., Badosa, J., Clain, G., Raux, C., and Vignelles, D.: Characterization and Corrections of Relative Humidity Measurement from Meteomodem M10 Radiosondes at Midlatitude Stations, J. Atmos. Ocean. Tech., 37, 857–871, https://doi.org/10.1175/JTECH-D-18-0205.1, 2020.

Gloeckner, H. M., Mieslinger, T., Robbins-Blanch, N., George, G., Kluft, L., Kölling, T., Bony, S., Windmiller, J., and Stevens, B.: BEACH: Barbados and Eastern Atlantic Combined High-altitude dropsonde datasets, Earth Syst. Sci. Data Discuss. [preprint], https://doi.org/10.5194/essd-2025-647, in review, 2025.

Hardy, B.: ITS-90 Formulations for Vapor Pressure, Frostpoint Temperature, Dewpoint Temperature, and Enhancement Factors in the Range −100 to +100 °C, in: Proceedings of the Third International Symposium on Humidity & Moisture, Teddington, London, UK, 1998.

Ingleby, B., Motl, M., Marlton, G., Edwards, D., Sommer, M., von Rohden, C., Vömel, H., and Jauhiainen, H.: On the quality of RS41 radiosonde descent data, Atmos. Meas. Tech., 15, 165–183, https://doi.org/10.5194/amt-15-165-2022, 2022.

Klocke, D., Wing, A., Segura, H., Dengler, M., Bell, M. M., Ruppert Jr., J. H., George, G., Kalesse-Los, H., Nuijens, L., Möller, K. O., Kiko, R., Mohr, W., Kidane, A. T., Trosits, A., Mertz, C., Imker, C., Begler, C., Blandfort, D., Colón-Burgos, D., Austen, D., Junyent, F., Schmidt, H., Habib, J., van der Giessen, J., Wieners, K.-H., Hayo, L., Stelzner, M., Lovato, M., O'Driscoll, O., Paschou, P., Henning, P., Mackenzie, R., Wimmer, W., Serikov, I., Brügmann, B., Wu, Y., Stevens, B., and Windmiller, J.: 40 days in the Rains: The inner life of the Atlantic ITCZ during BOWTIE, B. Am. Meteorol. Soc., submitted, 2026.

Lettau, H.: A Re-examination of the "Leipzig Wind Profile" Considering some Relations between Wind and Turbulence in the Frictional Layer, Tellus, 2, 125–129, https://doi.org/10.1111/j.2153-3490.1950.tb00321.x, 1950.

Mason, B. J.: The GARP Atlantic tropical experiment, Nature, 255, 17–20, https://doi.org/10.1038/255017a0, 1975.

Meteomodem: M20 radiosonde: Technical specifications and product information, Tech. rep., Meteomodem, Ury, France, http://leaflet.meteomodem.com/M20EN.pdf (last access: 9 March 2026), 2023.

Murphy, D. M. and Koop, T.: Review of the vapour pressures of ice and supercooled water for atmospheric applications, Q. J. Roy. Meteorol. Soc., 131, 1539–1565, https://doi.org/10.1256/qj.04.94, 2005.

Schulz, H. and Stevens, B.: Observing the Tropical Atmosphere in Moisture Space, J. Atmos. Sci., 75, 3313–3330, https://doi.org/10.1175/JAS-D-17-0375.1, 2018.

Schulz, H., Stolla, K., Köhler, L., Rixen, M., and Winkler, M.: pysonde: Postprocessing of Atmospheric Soundings (v0.0.7), Zenodo [code], https://doi.org/10.5281/zenodo.13831915, 2024.

Sonntag, D.: Fortschritte in der Hygrometrie, Meteorol. Z., 3, 51–66, https://doi.org/10.1127/metz/3/1994/51, 1994.

Stephan, C. C., Schnitt, S., Schulz, H., Bellenger, H., de Szoeke, S. P., Acquistapace, C., Baier, K., Dauhut, T., Laxenaire, R., Morfa-Avalos, Y., Person, R., Quiñones Meléndez, E., Bagheri, G., Böck, T., Daley, A., Güttler, J., Helfer, K. C., Los, S. A., Neuberger, A., Röttenbacher, J., Raeke, A., Ringel, M., Ritschel, M., Sadoulet, P., Schirmacher, I., Stolla, M. K., Wright, E., Charpentier, B., Doerenbecher, A., Wilson, R., Jansen, F., Kinne, S., Reverdin, G., Speich, S., Bony, S., and Stevens, B.: Ship- and island-based atmospheric soundings from the 2020 EUREC^{4}A field campaign, Earth Syst. Sci. Data, 13, 491–514, https://doi.org/10.5194/essd-13-491-2021, 2021.

Stevens, B., Farrell, D., Hirsch, L., Jansen, F., Nuijens, L., Serikov, I., Brügmann, B., Forde, M., Linne, H., Lonitz, K., and Prospero, J. M.: The Barbados Cloud Observatory: Anchoring Investigations of Clouds and Circulation on the Edge of the ITCZ, B. Am. Meteorol. Soc., 97, 787–801, https://doi.org/10.1175/BAMS-D-14-00247.1, 2016.

Stevens, B., Bony, S., David, R., Delanoë, J., Gross, S., Klocke, D., Windmiller, J., Wing, A., and Wu, Y.: ORCESTRA: Organized Convection and EarthCARE Studies over the Tropical Atlantic, Tellus, submitted, 2026.

Vaisala: White Paper: RS41 Radiosonde Performance, Tech. Rep. B211356EN-A, Vaisala Oyj, https://www.vaisala.com/sites/default/files/documents/RS41-White-Paper-B211356EN-A.pdf (last access: 3 August 2025), 2013.

Vaisala Oyj: RS41-SGP Radiosonde User's Guide, https://docs.vaisala.com/r/M211667DE-G/de-DE (last access: 13 August 2025), 2023.

Vaisala Oyj: RS41-SGPe Radiosonde User's Guide, https://docs.vaisala.com/r/M212917EN-B/en-US (last access: 13 August 2025), 2024.

Venkiteshwaran, S.: The F-type radio-meteorograph as an instrument to measure vertical currents in the atmosphere, Proc. Indian Acad. Sci.-Sect. A, 35, 281–289, 1952.

Wagner, W. and Pruß, A.: The IAPWS Formulation 1995 for the Thermodynamic Properties of Ordinary Water Substance for General and Scientific Use, J. Phys. Chem. Ref. Data, 31, 387–535, https://doi.org/10.1063/1.1461829, 2002.

Wagner, W., Riethmann, T., Feistel, R., and Harvey, A. H.: New Equations for the Sublimation Pressure and Melting Pressure of H_2O Ice Ih, J. Phys. Chem. Ref. Data, 40, 043103, https://doi.org/10.1063/1.3657937, 2011.

Winkler, M. and Rixen, M.: RAPSODI Radiosonde Measurements during ORCESTRA (Level 1) (merged, padded to common vertical levels), ORCESTRA [data set], https://doi.org/10.82246/BAFYBEIA34AUWYVBH2RQ7CN7, 2026a.

Winkler, M. and Rixen, M.: RAPSODI Radiosonde Measurements during ORCESTRA (Level 2), ORCESTRA [data set], https://doi.org/10.82246/BAFYBEID7CNW62ZMZFGXCVC6, 2026b.

Winkler, M., Rixen, M., Beucher, F., Couvreux, F., Nam, C. C., Peyrillé, P., Schmidt, H., Segura, H., Wieners, K.-H., Alkilani-Brown, E., Coly, A. A., Biagioli, G., Bell, M. M., Brito, E., Chauvin, E., Capo, J., Colón-Burgos, D., Dawes, A., da Luz, J. C., Demiralay, Z., Douet, V., Ducastin, V., Dufaux, C., Dufresne, J.-L., Favot, F., Fiolleau, T., Fons, E., George, G., Gloeckner, H. M., Gonçalves, S., Gouttesoulard, L., Hayo, L., Hsiao, W.-T.,

Kennison, S., Kopelman, M., Lee, T.-Y., Le Gall, E., Lovato, M., Luschen, E., Maury, N., McKim, B., Netz, L., Ousseynou, D., Peters-von Gehlen, K., Pope, C., Poujol, B., Rivera Maldonado, N., Robbins-Blanch, N., Rochetin, N., Rowe, D., Romero Jure, P., Ruppert Jr., J. H., Segura Bermudez, J., Starr, J. C., Stelzner, M., Stoll, C., Syrett, M., Tekoe, A., Trules, J., Welty, C., Klocke, D., Vogel, R., Bony, S., Wing, A. A., and Stevens, B.: RAPSODI: Radiosonde Atmospheric Profiles from Ship and island platforms during ORCESTRA, collected to Decipher the ITCZ, Earth Syst. Sci. Data Discuss. [preprint], https://doi.org/10.5194/essd-2025-638, in review, 2025a.

Winkler, M., Rixen, M., Beucher, F., Couvreux, F., Nam, C. C., Peyrillé, P., Schmidt, H., Segura, H., Wieners, K.-H., Alkilani-Brown, E., Coly, A. A., Biagioli, G., Bell, M. M., Brito, E., Chauvin, E., Capo, J., Colón-Burgos, D., Dawes, A., Carlos da Luz, J., Demiralay, Z., Douet, V., Ducastin, V., Dufaux, C., Dufresne, J.-L., Favot, F., Fiolleau, T., Fons, E., George, G., Gloeckner, H. M., Gonçalves, S., Gouttesoulard, L., Hayo, L., Hsiao, W.-T., Kennison, S., Kopelman, M., Lee, T.-Y., Le Gall, E., Lovato, M., Luschen, E., Maury, N., McKim, B., Netz, L., Ousseynou, D., Peters-von Gehlen, K., Pope, C., Poujol, B., Rivera Maldonado, N., Robbins-Blanch, N., Rochetin, N., Rowe, D., Romero Jure, P., Ruppert Jr., J. H., Segura Bermudez, J., Starr, J. C., Stelzner, M., Stoll, C., , Syrett, M., Tekoe, A., Trules, J., Welty, C., Klocke, D., Vogel, R., Bony, S., Wing, A. A., and Stevens, B.: RAPSODI Raw Radiosonde Measurements during ORCESTRA (Level 0, BCO), ORCESTRA [data set], https://ipfs.io/ipns/latest.orcestra-campaign.org/raw/BCO/radiosondes/, (last access: 9 March 2026), 2025b.

Winkler, M., Rixen, M., Beucher, F., Couvreux, F., Nam, C. C., Peyrillé, P., Schmidt, H., Segura, H., Wieners, K.-H., Alkilani-Brown, E., Coly, A. A., Biagioli, G., Bell, M. M., Brito, E., Chauvin, E., Capo, J., Colón-Burgos, D., Dawes, A., Carlos da Luz, J., Demiralay, Z., Douet, V., Ducastin, V., Dufaux, C., Dufresne, J.-L., Favot, F., Fiolleau, T., Fons, E., George, G., Gloeckner, H. M., Gonçalves, S., Gouttesoulard, L., Hayo, L., Hsiao, W.-T., Kennison, S., Kopelman, M., Lee, T.-Y., Le Gall, E., Lovato, M., Luschen, E., Maury, N., McKim, B., Netz, L., Ousseynou, D., Peters-von Gehlen, K., Pope, C., Poujol, B., Rivera Maldonado, N., Robbins-Blanch, N., Rochetin, N., Rowe, D., Romero Jure, P., Ruppert Jr., J. H., Segura Bermudez, J., Starr, J. C., Stelzner, M., Stoll, C., , Syrett, M., Tekoe, A., Trules, J., Welty, C., Klocke, D., Vogel, R., Bony, S., Wing, A. A., and Stevens, B.: RAPSODI Raw Radiosonde Measurements during ORCESTRA (Level 0, INMG), ORCESTRA [data set], https://ipfs.io/ipns/latest.orcestra-campaign.org/raw/INMG/radiosondes/ (last access: 9 March 2026), 2025c.

Winkler, M., Rixen, M., Beucher, F., Couvreux, F., Nam, C. C., Peyrillé, P., Schmidt, H., Segura, H., Wieners, K.-H., Alkilani-Brown, E., Coly, A. A., Biagioli, G., Bell, M. M., Brito, E., Chauvin, E., Capo, J., Colón-Burgos, D., Dawes, A., Carlos da Luz, J., Demiralay, Z., Douet, V., Ducastin, V., Dufaux, C., Dufresne, J.-L., Favot, F., Fiolleau, T., Fons, E., George, G., Gloeckner, H. M., Gonçalves, S., Gouttesoulard, L., Hayo, L., Hsiao, W.-T., Kennison, S., Kopelman, M., Lee, T.-Y., Le Gall, E., Lovato, M., Luschen, E., Maury, N., McKim, B., Netz, L., Ousseynou, D., Peters-von Gehlen, K., Pope, C., Poujol, B., Rivera Maldonado, N., Robbins-Blanch, N., Rochetin, N., Rowe, D., Romero Jure, P., Ruppert Jr., J. H., Segura Bermudez, J., Starr, J. C., Stelzner, M., Stoll, C., , Syrett, M., Tekoe, A., Trules, J., Welty, C., Klocke, D., Vogel, R., Bony, S., Wing, A. A., and Stevens, B.: RAPSODI Raw Radiosonde Measurements during ORCESTRA (Level 0, R/V *Meteor*), ORCESTRA [data set], https://ipfs.io/ipns/latest.orcestra-campaign.org/raw/METEOR/radiosondes/ (last access: 9 March 2026), 2025d.

Winkler, M., Wieners, K.-H., and Rixen, M.: RAPSODI Oscillating Radiosonde Measurements during ORCESTRA (Level 1), ORCESTRA [data set], https://doi.org/10.82246/BAFYBEIHXRAJOJUQZYX65QSO7, 2026.